scientific reports

Check for updates

OPEN

Identification of candidate biomarkers and pathways associated with type 1 diabetes mellitus using bioinformatics analysis

Madhu Pujar[1], Basavaraj Vastrad[2], Satish Kavatagimath[3], Chanabasayya Vastrad[4]✉ & Shivakumar Kottursheti[4]

Type 1 diabetes mellitus (T1DM) is a metabolic disorder for which the underlying molecular mechanisms remain largely unclear. This investigation aimed to elucidate essential candidate genes and pathways in T1DM by integrated bioinformatics analysis. In this study, differentially expressed genes (DEGs) were analyzed using DESeq2 of R package from GSE162689 of the Gene Expression Omnibus (GEO). Gene ontology (GO) enrichment analysis, REACTOME pathway enrichment analysis, and construction and analysis of protein–protein interaction (PPI) network, modules, miRNA-hub gene regulatory network and TF-hub gene regulatory network, and validation of hub genes were performed. A total of 952 DEGs (477 up regulated and 475 down regulated genes) were identified in T1DM. GO and REACTOME enrichment result results showed that DEGs mainly enriched in multicellular organism development, detection of stimulus, diseases of signal transduction by growth factor receptors and second messengers, and olfactory signaling pathway. The top hub genes such as MYC, EGFR, LNX1, YBX1, HSP90AA1, ESR1, FN1, TK1, ANLN and SMAD9 were screened out as the critical genes among the DEGs from the PPI network, modules, miRNA-hub gene regulatory network and TF-hub gene regulatory network. Receiver operating characteristic curve (ROC) analysis confirmed that these genes were significantly associated with T1DM. In conclusion, the identified DEGs, particularly the hub genes, strengthen the understanding of the advancement and progression of T1DM, and certain genes might be used as candidate target molecules to diagnose, monitor and treat T1DM.

Type 1 diabetes mellitus (T1DM) is chronic autoimmune diabetes characterized by autoimmune mediated destruction of pancreatic beta cells[1]. T1DM is most generally identified in children and adolescents[2]. Epidemiological studies have shown that the incidence of T1DM has been increasing by 2–5% globally[3]. T1DM is a complex disease affected by numerous environmental factors, genetic factors and their interactions[4,5]. Several T1DM associated complications include cardiovascular disease[6], hypertension[7], diabetic retinopathy[8], diabetic nephropathy[9], diabetic neuropathy[10], obesity[11] and cognitive impairment[12]. Therefore, it is crucial to understand the precise molecular mechanisms associated in the progression of T1DM and thus establish effective diagnostic, prognostics and therapeutic strategies.

Although the remarkable improvement is achieved in the treatment of T1DM is insulin therapy[13], the long-term survival rates of T1DM still remain low worldwide. One of the major reasons is that most patients with T1DM were diagnosed at advanced stages. It is crucial to find out novel diagnostic biomarkers, prognostic biomarkers and therapeutic targets for the early diagnosis, prognosis and timely treatment of T1DM. Therefore, it is still urgent to further explore the exact molecular mechanisms of the development of T1DM. At present, several genes and signaling pathway are identified; for example vitamin D receptor (VDR)[14], HLA-B and

[1]Department of Pediatrics, J J M Medical College, Davangere, Karnataka 577004, India. [2]Department of Pharmaceutical Chemistry, K.L.E. College of Pharmacy, Gadag, Karnataka 582101, India. [3]Department of Pharmacognosy, K.L.E. College of Pharmacy, Belagavi, Karnataka 590010, India. [4]Biostatistics and Bioinformatics, Chanabasava Nilaya, Bharthinagar, Dharwad, Karnataka 580001, India. ✉email: channu.vastrad@gmail.com

HLA-A[15], HLA-DQ[16], HLA-DQB1, HLA-DQA1 and HLA-DRB1[17], IDDM2[18], CaMKII/NF-κB/TGF-β1 and PPAR-γ signaling pathway[19], Keap1/Nrf2 signaling pathway[20], HIF-1/VEGF pathway[21], NLRP3 and NLRP1 inflammasomes signaling pathway[22] and NO/cGMP signaling pathway[23]. Therefore, it is crucial to examine the accurate molecular targets included in occurrence and advancement of T1DM, in order to make a contribution to the diagnosis and treatment of T1DM.

Next generation sequencing (NGS) platform for gene expression analysis have been increasingly recognized as approaches with significant clinical value in areas such as molecular diagnosis, prognostic prediction and identification of novel therapeutic targets[24]. In recent years, NGS data analysis has been effective in detecting the advancement of T1DM, and even in screening biomarkers for T1DM prognosis, diagnosis and therapy. We therefore used an NGS dataset to investigate the molecular pathogenesis of T1DM.

In the present investigation, we selected NGS dataset GSE162689[25], from Gene Expression Omnibus database (GEO) (http://www.ncbi.nlm.nih.gov/geo/)[26] and used the DESeq2 package in R software to screen DEGs. We performed subsequent bioinformatics analysis, including gene ontology (GO) enrichment and REACTOME pathway enrichment analysis, and construction and analysis of protein–protein interaction (PPI) network, module analysis, construction and analysis of miRNA-hub gene regulatory network and TF-hub gene regulatory network. The hub genes were validated by receiver operating characteristic curve (ROC) analysis. This investigation might offer better insight into potential molecular mechanisms to examine preventive and therapeutic strategies.

Materials and methods

Data resources. NGS dataset of T1DM (GSE162689)[25] was downloaded from the GEO database. The GSE162689 NGS data was composed of 27 T1DM samples and 32 normal control samples was based on the GPL24014 Ion Torrent S5 XL (Homo sapiens).

Identification of DEGs. Differentially expressed genes (DEGs) between T1DM and normal control samples were identified by using the DESeq2 package in R language software[27]. DEGs were considered when an adjusted $P < 0.05$, and a $|\log2 \text{ fold change}| > 0.63$ for up regulated genes and $|\log2 \text{ fold change}| < -1.3$ for down regulated genes. The adjusted P values, by employing Benjamini and Hochberg false discovery rate[28], were aimed to correct the occurrence of false positive results. The DEGs were presented in volcano plot and heat map drawn using a plotting tool ggplot2 and gplots based on the R language.

GO and REACTOME pathway enrichment analysis of DEGs. One online tool, g:Profiler (http://biit.cs.ut.ee/gprofiler/)[29], was applied to carried out the functional annotation for DEGs. Gene Ontology (GO) (http://geneontology.org/)[30] generally performs enrichment analysis of genomes. GO terms includes biological processes (BP), cellular components (CC) and molecular functions (MF) in the GO enrichment analysis. REACTOME (https://reactome.org/)[31] is a comprehensive database of genomic, chemical, and systemic functional information. GO and pathway enrichment analyses were used to identify the significant GO terms and pathways. $P < 0.05$ was set as the cutoff criterion.

Construction of the PPI network and module analysis. PPI network was established using the IntAct Molecular Interaction Database (https://www.ebi.ac.uk/intact/)[32]. To assess possible PPI correlations, previously identified DEGs were mapped to the IntAct database, followed by extraction of PPI pairs with a combined score > 0.4. Cytoscape 3.8.2 software (www.cytoscape.org/)[33] was then employed to visualize the PPI network, and the Cytoscape plugin Network Analyzer was used to calculate the node degree[34], betweenness centrality[35], stress centrality[36] and closeness centrality[37] of each node in PPI network. Specifically, nodes with a higher node degree, betweenness centrality, stress centrality and closeness centrality were likely to play a more vital role in maintaining the stability of the entire network. The PEWCC1 (http://apps.cytoscape.org/apps/PEWCC1)[38] plug-in was applied to analyze the modules in the PPI networks, with the default parameters (node score = 0.2, K-core $\geqq$ 2, and max depth = 100).

MiRNA-hub gene regulatory network construction. The miRNAs targeting the T1DM related were predicted using the miRNet database (https://www.mirnet.ca/)[39], and those predicted by at least 14 databases (TarBase, miRTarBase, miRecords, miRanda, miR2Disease, HMDD, PhenomiR, SM2miR, PharmacomiR, EpimiR, starBase, TransmiR, ADmiRE, and TAM 2.0) were selected for constructing the miRNA-hub gene regulatory network by Cytoscape 3.8.2 software[33].

TF-hub gene regulatory network construction. The TFs targeting the T1DM related were predicted using the NetworkAnalyst database (https://www.networkanalyst.ca/)[40], and those predicted by RegNetwork database was selected for constructing the TF-hub gene regulatory network by Cytoscape 3.8.2 software[33].

Validation of hub genes by receiver operating characteristic curve (ROC) analysis. A ROC curve analysis is an approach for visualizing, organizing and selecting classifiers based on their achievement of hub genes. A diagnostic test was firstly performed in order to estimate the diagnostic value of hub genes in T1DM. ROC curves were obtained by plotting the sensitivity, against the specificity using the R package "pROC"[41]. Area under the curve (AUC) was used to measure the accuracy of these diagnostic values of the hub genes An AUC > 0.9 determined that the model had a favorable fitting effect.

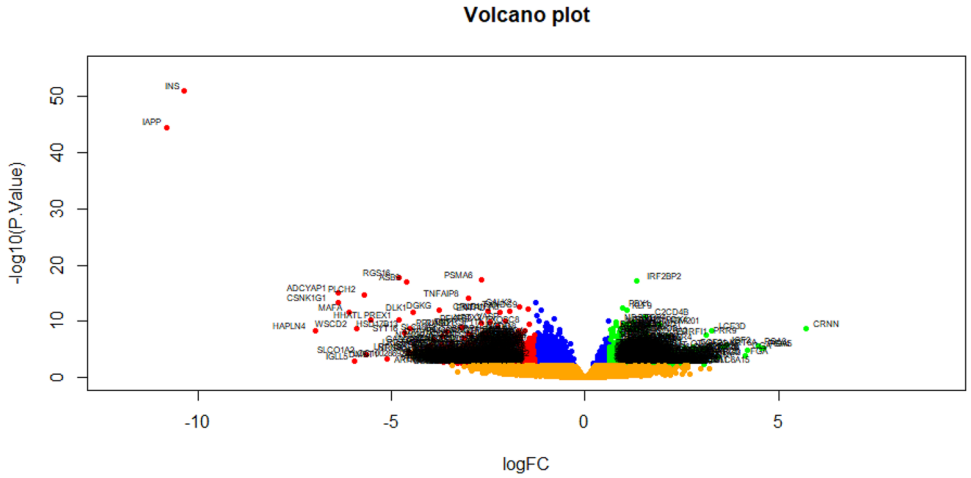

Figure 1. Volcano plot of differentially expressed genes. Genes with a significant change of more than two-fold were selected. Green dot represented up regulated significant genes and red dot represented down regulated significant genes.

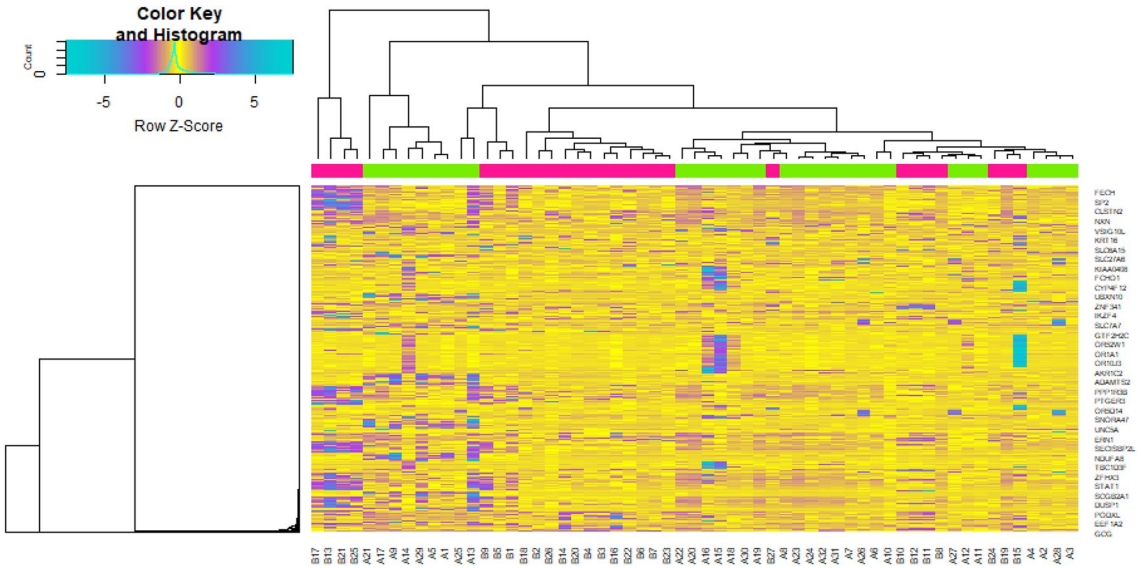

Figure 2. Heat map of differentially expressed genes. Legend on the top left indicate log fold change of genes. (A1–A32 = normal control samples; B1–B27 = T1DM samples).

Ethical approval. This article does not contain any studies with human participants or animals performed by any of the authors.

Informed consent. No informed consent because this study does not contain human or animals participants.

Results

Identification of DEGs. On the basis of the cut-off criteria, DEGs in GEO dataset was identified between T1DN and normal control samples (Supplementary Table S1). There were 952 DEGs, including 477 up regulated and 475 down regulated genes in GSE162689 with the threshold of adjusted $P < 0.05$, and a |log2 fold change|> 0.63 for up regulated genes and |log2 fold change|< -1.3 for down regulated genes. Volcano plots (Fig. 1) showed the correlation of all DEGs from the NGS data. Heat map of the up regulated and down regulated genes were indicated in Fig. 2.

GO and REACTOME pathway enrichment analysis of DEGs. To characterize the functional roles of the above DEGs, we used GO (Table 1) and REACTOME pathway (Table 2) enrichment analyses. The BP category of the GO analysis results showed that up regulated genes were significantly enriched in multicellular

GO ID	CATEGORY	GO name	Adjusted p value	Negative log10 of adjusted p value	Gene count	Gene
Up regulated genes						
GO:0007275	BP	Multicellular organism development	1.03027E−05	4.987047489	192	IGF2, KRT6A, LCE3D, SPRR3, FLG, SPRR2D, SPRR1B, SLITRK6, FGF21, TBX22, CALCR, SPRR1A, USH2A, OTX2, DCC, KCP, NOG, STAR, KRT16, IL1RN, SHISA2, AQP5, SYNDIG1, TFAP2C, ERRFI1, PLP1, ALOX12, KRT13, SPRR2E, TENM1, PEMT, LY6H, FAP, EYA4, LCE3E, EGR1, CSGALNACT1, MAL, MMP16, PTGER4, COL6A3, OAS2, ETV4, MAOB, GPC6, SOCS5, BCL9, POU6F2, BTG2, PRR15, VEGFC, FAM20C, MPZ, TMEM176A, KLK13, RPS6, ID3, ALOXE3, DDIT4, IRF2BP2, KLF15, EGR3, RNF165, LTBP4, CREB3L1, EMX1, KLF3, ZFP36, QDPR, ETV5, KL, GADD45B, NXN, TLE3, HEYL, HRAS, GLI3, SFTPD, MYC, IGSF8, DMD, FKBP8, DBP, MTCH1, KLF10, PODXL, BVES, MNT, LSR, CEL, FOSL2, WASF1, PAPSS2, NR1D1, DUSP4, SNX19, FOXN3, IL6ST, IL6R, PCDHB6, KLF6, ZFP36L1, PBX1, SH3RF1, CNTN3, NHEJ1, BOC, STAT1, DUSP1, CLSTN2, DIP2B, MYADM, PCDHB11, APOD, NR0B2, NHS, SYVN1, TCF7L2, DLL4, NNMT, SMAD1, TP53, PCDH18, SUN2, SOS1, PRKACA, EGFR, ETS1, PIK3CA, TSHZ1, GCNT2, PKN1, TNFRSF1A, ELOVL1, NCSTN, MFAP2, YBX1, PLCE1, NDST1, KCNJ8, GAMT, DGCR2, TPI1, JMJD8, NES, WDTC1, MAML1, PCDHB4, NFIB, MAPK3, SLC23A2, FOXK1, CAMSAP3, ACVR2B, PLOD3, ZFHX3, SMURF1, PRMT6, PRKCSH, ETV6, GSK3A, WDR74, BCOR, NPAS2, USP1, RBM47, RNF43, TCOF1, NCL, METTL14, KCTD11, HSP90AA1, BTG1, GAB1, S1PR1, THRB, EDNRB, SYBU, CDNF, MEX3C, SIAH2, NFKBIA, GJA1, CD34, DEAF1, INSR, NR1D2, GADD45G, ZNRF3, MBOAT7, BSG, BTF3
GO:0006807	BP	Nitrogen compound metabolic process	8.09009E−05	4.092046627	292	CRNN, PGA5, CGA, FGA, IGF2, FGB, APOA5, SPRR3, FLG, SPRR1B, FGF21, FGG, TBX22, CALCR, PGC, SPRR1A, ABCB11, OTX2, MUC21, NOG, HSFX2, ZSCAN10, TFAP2C, ERRFI1, RUNX1T1, ALOX12, SPRR2E, PDK4, TENM1, HAO1, PEMT, FAP, EYA4, ZNF554, EGR1, CSGALNACT1, GCG, MMP16, ADAMTS8, COL6A3, MAPK4, OAS2, ETV4, MAOB, GPC6, SOCS5, GMNC, BCL9, PDK3, POU6F2, BTG2, A4GNT, CST6, VEGFC, FAM20C, USP27X, STK32B, KLK13, RPS6, ID3, PGAP2, ALOXE3, LSM11, BCAP31, DDIT4, DPP4, TYSND1, IRF2BP2, KLF15, EGR3, RNF165, PHLDA1, LTBP4, IKZF4, CREB3L1, A1CF, EMX1, NAT10, ACSL6, KLF3, ZFP36, QDPR, OAS1, ETV5, GADD45B, MAN1A1, NXN, TLE3, RPL8, HEYL, PER3, HRAS, GLI3, SFTPD, MYC, RPRD2, DMD, ZNF416, FKBP8, RPS28, DBP, MUC6, MTCH1, CHST10, KLF9, EIF4B, KLF10, GLTP, MNT, CEL, NUP205, FOSL2, ZNF362, PAPSS2, NR1D1, DUSP4, SMCR8, FECH, FOXN3, IL6ST, IL6R, ZNF581, KLF6, CPA1, ABCA1, ZFP36L1, PBX1, SH3RF1, URM1, ERN1, RPL18, RNF24, PRRC1, NHEJ1, PDK2, STAT1, HSPA2, DUSP1, DIP2B, FMOD, MYADM, APOD, GLS, FBXO32, SRM, DIRAS3, NR0B2, SYVN1, ARL6IP1, TCF7L2, TMUB1, MRPL37, DLL4, HELZ2, NNMT, SMAD1, TP53, ELK1, PTBP1, PRKACA, BACH2, CTSF, EGFR, ETS1, PIK3CA, ZNRF1, CMPK2, GUK1, TSHZ1, ZNF326, MED13L, GCNT2, SAE1, PKN1, TNFRSF1A, ELOVL1, TUT1, NCSTN, YBX1, PPP1R3B, PLCE1, NDST1, ATF6B, GAMT, TPI1, JMJD8, SECISBP2L, PRPF8, EIF3B, WDTC1, MAML1, CRNKL1, NFIB, MAPK3, RPL18A, CNDP2, SERTAD2, RCE1, FOXK1, ZNF646, ACVR2B, PLOD3, ZFHX3, SMURF1, AOX1, RPS15, PRMT6, TRIM24, PRKCSH, ETV6, GSK3A, WDR74, LARP6, BCOR, URB1, ZNF341, SGTA, STUB1, NPAS2, MAOA, USP1, RBM47, RNF43, SHISA5, TCOF1, NCL, FKBP5, RBM22, METTL14, PIGM, ATF7IP, POLR1D, UBAP2, UBE2E2, SPPL3, KCTD11, HSP90AA1, BTG1, S1PR1, THRB, RPL39, UTP14A, EDNRB, CRTC3, AK1, MED25, ERP29, RBM23, RNASEK, LPCAT3, CASC3, MTMR3, TNKS, SF3A1, ADPRHL1, MEX3C, SIAH2, ACD, NFKBIA, GJA1, RNPS1, ATP13A2, TXNDC5, MRPL49, SLC35C2, CD34, SQSTM1, DEAF1, INSR, RPL19, NR1D2, AGBL5, SP2, SLC2A4RG, MRPS18B, NEDD9, GADD45G, ZNRF3, MAST3, SNX12, BAZ2A, MBOAT7, GID8, DCPS, LIG3, SP4, KLF11, CIZ1, LNX1, RALB, BTF3, ZNF836
GO:0031974	CC	Membrane-enclosed lumen	0.000311835	3.506075034	175	PGA5, CGA, FGA, IGF2, FGB, APOA5, FGG, MUC21, STAR, ZSCAN10, TFAP2C, RUNX1T1, SLC7A14, PDK4, TENM1, HAO1, ZNF554, EGR1, GCG, MMP16, COL6A3, MAPK4, OAS2, ETV4, GPC6, BCL9, PDK3, VEGFC, FAM20C, RPS6, LSM11, TYSND1, IRF2BP2, KLF15, PHLDA1, IKZF4, A1CF, EMX1, NAT10, KLF3, OAS1, ETV5, GRIK5, GPR63, TLE3, HEYL, HRAS, GLI3, MYC, RPRD2, IRS1, RPS28, MUC6, KLF9, PODXL, MNT, NUP205, FOSL2, NR1D1, DUSP4, SMCR8, FECH, KLF6, PBX1, RPL18, ABCG2, NHEJ1, PDK2, SELENBP1, STAT1, HSPA2, FMOD, GLS, FBXO32, NR0B2, NHS, SYVN1, TCF7L2, TMUB1, MRPL37, HELZ2, SMAD1, TP53, ELK1, SUN2, PTBP1, PRKACA, BACH2, TOR2A, CTSF, EGFR, ETS1, CMPK2, C17ORF49, ZNF326, SAE1, PKN1, TUT1, YBX1, ME2, JMJD8, PRPF8, WDTC1, MAML1, CRNKL1, NFIB, MAPK3, CNDP2, SERTAD2, FOXK1, CAMSAP3, PLOD3, FAM193B, ZFHX3, SMURF1, RPS15, PRMT6, TRIM24, PRKCSH, ETV6, WDR74, BCOR, URB1, STUB1, NPAS2, USP1, SHISA5, TCOF1, NCL, FKBP5, RBM22, METTL14, MZT2B, ATF7IP, POLR1D, FIGN, HSP90AA1, BTG1, S1PR1, THRB, UTP14A, CRTC3, MED25, ERP29, CASC3, TNKS, SF3A1, CHID1, SIAH2, ACD, NFKBIA, ARHGAP17, GJA1, RNPS1, ATP13A2, TXNDC5, MRPL49, SLC35C2, SQSTM1, DEAF1, INSR, RPL19, NR1D2, SP2, SLC2A4RG, MRPS18B, NEDD9, BAZ2A, CCDC86, GID8, DCPS, LIG3, SP4, KLF11, CIZ1
GO:0031981	CC	nuclear lumen	0.004404749	2.356078816	139	ZSCAN10, TFAP2C, RUNX1T1, SLC7A14, TENM1, ZNF554, EGR1, MAPK4, OAS2, ETV4, BCL9, PDK3, RPS6, LSM11, IRF2BP2, KLF15, PHLDA1, IKZF4, A1CF, EMX1, NAT10, KLF3, OAS1, ETV5, GRIK5, GPR63, TLE3, HEYL, HRAS, GLI3, MYC, RPRD2, IRS1, RPS28, KLF9, PODXL, MNT, NUP205, FOSL2, NR1D1, DUSP4, SMCR8, KLF6, PBX1, RPL18, ABCG2, NHEJ1, PDK2, SELENBP1, STAT1, HSPA2, FBXO32, NR0B2, NHS, SYVN1, TCF7L2, TMUB1, HELZ2, SMAD1, TP53, ELK1, SUN2, PTBP1, PRKACA, BACH2, ETS1, CMPK2, C17ORF49, ZNF326, SAE1, PKN1, TUT1, YBX1, PRPF8, WDTC1, MAML1, CRNKL1, NFIB, MAPK3, CNDP2, SERTAD2, FOXK1, CAMSAP3, FAM193B, ZFHX3, SMURF1, RPS15, PRMT6, TRIM24, ETV6, WDR74, BCOR, URB1, STUB1, NPAS2, USP1, TCOF1, NCL, FKBP5, RBM22, METTL14, MZT2B, ATF7IP, POLR1D, FIGN, HSP90AA1, BTG1, S1PR1, THRB, UTP14A, CRTC3, MED25, CASC3, TNKS, SF3A1, SIAH2, ACD, NFKBIA, ARHGAP17, GJA1, RNPS1, SLC35C2, SQSTM1, DEAF1, INSR, RPL19, NR1D2, SP2, SLC2A4RG, MRPS18B, NEDD9, BAZ2A, CCDC86, GID8, DCPS, LIG3, SP4, KLF11, CIZ1

Continued

GO ID	CATEGORY	GO name	Adjusted p value	Negative log10 of adjusted p value	Gene count	Gene
GO:0005515	MF	Protein binding	0.010406822	1.982681882	384	CRNN, CGA, FGA, IGF2, KRT6A, FGB, LCE3D, SLC6A15, APOA5, SPRR3, FLG, SLITRK6, FGF21, FGG, TBX22, CALCR, SPRR1A, ABCB11, USH2A, OTX2, HBM, DCC, POTED, KCP, RGPD3, NOG, STAR, KRT16, HSFX2, IL1RN, ZSCAN10, SHISA2, TACR1, AQP5, SYNDIG1, TFAP2C, ERRFI1, TMEM174, CNTNAP4, PLP1, RUNX1T1, ALOX12, KRT13, SLC7A14, SPRR2E, PDK4, TENM1, PRLHR, SLC22A11, PEMT, LY6H, TMEM236, FAP, EYA4, BTBD11, FBP2, LCE3E, ZNF554, EGR1, CSGALNACT1, MT2A, MAL, SLC38A4, GCG, ASIC1, ADAMTS8, PTGER4, TMEM201, COL6A3, MAPK4, OAS2, AQP7, SLC25A48, ETV4, MAOB, GPC6, KCNJ2, MT1E, SOCS5, GMNC, BCL9, PDK3, ABCC9, POU6F2, BTG2, CST6, PRR15, VEGFC, FAM20C, C16ORF89, TMEM176A, KLK13, RPS6, ID3, PGAP2, ALOXE3, LSM11, BCAP31, DDIT4, DPP4, TYSND1, KLF15, RNF165, AQP8, SLC22A17, PHLDA1, FAM86B2, LTBP4, IKZF4, CREB3L1, A1CF, EMX1, NAT10, NETO2, ACSL6, KLF3, ZFP36, QDPR, OAS1, ETV5, GRIK5, KL, ZNF385C, GADD45B, SLC29A3, CGREF1, TLE3, RPL8, HEYL, PER3, HRAS, GLI3, WDR89, KIAA0408, SFTPD, MYC, TTI1, IFIT3, IGSF8, RPRD2, DMD, AQP12B, FKBP8, IRS1, KIAA1958, RPS28, TMEM140, MUC6, MTCH1, ABHD15, EIF4B, KLF10, PODXL, BVES, GLTP, MNT, CEL, NUP205, FOSL2, SLC1A5, WASF1, PAPSS2, TMCO4, NR1D1, DUSP4, SNX19, SMCR8, FECH, FOXN3, IL6ST, IL6R, PCDHB6, ZNF581, KLF6, CPA1, ABCA1, ZFP36L1, PBX1, DYSF, SH3RF1, PLEKHG6, URM1, ERN1, RPL18, CNTN3, CYGB, RNF24, ABCG2, PRRC1, NHEJ1, PDK2, BOC, SELENBP1, STAT1, HSPA2, DUSP1, DIP2B, FMOD, MYADM, ARPC1A, KCTD12, APOD, GLS, FBXO32, SRM, DIRAS3, NR0B2, SYVN1, ARL6IP1, TCF7L2, TMUB1, DHRS11, DL14, HELZ2, SMAD1, TP53, PCDH18, ELK1, SUN2, TMEM150A, PTBP1, SOS1, PRKACA, BACH2, TOR2A, EGFR, ETS1, PIK3CA, ZNRF1, C17ORF49, GUK1, ZNF326, GCNT2, SAE1, GTPBP8, PKN1, TNFRSF1A, ELOVL1, TUT1, NCSTN, MFAP2, YBX1, PPP1R3B, PLCE1, NDST1, KCNJ8, ATF6B, GAMT, DGCR2, TPI1, JMJD8, NES, CDC42EP3, SECISBP2L, PRPF8, DNAJC4, EIF3B, EPHX1, WDTC1, MAML1, CRNKL1, MAPK3, RPL18A, FAM83B, SERTAD2, FOXK1, ZNF646, CAMSAP3, ACVR2B, ATXN7L1, LRRC8B, PLOD3, FAM193B, ZFHX3, SMURF1, AOX1, RPS15, PRMT6, TRIM24, PRKCSH, ETV6, GSK3A, WDR74, KCNC4, LARP6, BCOR, PSD4, RAB4A, ZNF341, SGTA, STUB1, SLC35E1, NPAS2, MAOA, USP1, RBM47, RNF43, KIAA0930, SHISA5, TCOF1, NCL, FKBP5, RBM22, SLC48A1, TRAPPC3, METTL14, MZT2B, ATF7IP, RWDD2B, POLR1D, UBIAD1, SFXN2, FIGN, UBAP2, UBE2E2, MX1, SPPL3, KCTD11, HSP90AA1, BTG1, GAB1, PXMP2, S1PR1, THRB, UTP14A, EDNRB, CRTC3, SYBU, MED25, ERP29, RBM23, CDNF, RNASEK, CASC3, MTMR3, TNKS, SF3A1, CHID1, AGPAT3, MEX3C, SIAH2, ACD, NFKBIA, CDC42EP4, ARHGAP17, GJA1, RNPS1, ATP13A2, ZSWIM3, TXNDC5, PPFIBP2, MRPL49, SLC35C2, CD34, SQSTM1, DEAF1, CPNE8, INSR, RPL19, NR1D2, AGBL5, SP2, YIPF3, MRPS18B, NEDD9, GADD45G, ZNRF3, MAST3, SNX12, TMED5, BAZ2A, CCDC86, MBOAT7, GID8, DCPS, LIG3, BSG, SP4, KLF11, CIZ1, LNX1, RALB, BTF3, NET1
GO:0140110	MF	Transcription regulator activity	0.019982707	1.699345683	71	TBX22, OTX2, HSFX2, ZSCAN10, TFAP2C, RUNX1T1, ZNF554, EGR1, ETV4, BCL9, POU6F2, BTG2, IRF2BP2, KLF15, EGR3, IKZF4, CREB3L1, EMX1, KLF3, ETV5, TLE3, HEYL, GLI3, MYC, ZNF416, DBP, KLF9, KLF10, MNT, FOSL2, ZNF362, NR1D1, FOXN3, ZNF581, KLF6, PBX1, STAT1, NR0B2, TCF7L2, HELZ2, SMAD1, TP53, ELK1, BACH2, ETS1, TSHZ1, MED13L, PKN1, ATF6B, MAML1, NFIB, SERTAD2, FOXK1, ZNF646, ZFHX3, TRIM24, ETV6, BCOR, ZNF341, NPAS2, ATF7IP, BTG1, THRB, SIAH2, DEAF1, NR1D2, SP2, SLC2A4RG, SP4, KLF11, ZNF836
Down regulated genes						
GO:0051606	BP	Detection of stimulus	9.55E−21	20.01997014	63	DMBT1, OR10J3, OR4F5, OR6C74, OR5L1, OR4D2, OR2T33, OR2T6, GJA10, OR8H2, OR4N2, CASQ2, OR2A25, TAS2R7, OR1E2, OR2B3, OR6N1, OR4K5, OR4A5, OR5AN1, OR5AS1, OR13G1, OR2M5, OR13C5, OR4C3, OR52L1, OR8K1, OR6R2, OR56A4, OR5B17, OR51A2, OR5T1, OR1A1, OR13C8, OR13C2, OR51B4, OR2AG2, OR2M7, OR51L1, OR5H1, OR8G1, OR6K6, OR10Z1, OR4K1, OR5T2, OR2A12, OR1L8, OR1J2, TAS2R60, CHRNA10, OR5AP2, OR52K1, OR9A2, OR10A5, OR4C46, OR52W1, TAS2R8, OR52E6, TTN, OR6K3, OR11H2, OR52D1, PKDREJ
GO:0032501	BP	Multicellular organismal process	3.26E−07	6.486491268	224	IAPP, HAPLN4, ADCYAP1, DMBT1, RGS16, PREX1, NRG3, LRRTM3, GABRA2, GTSF1, NTNG2, GLRA1, DGKG, ISX, OR10J3, SLC6A17, DACH2, IFNA16, OR4F5, SLC18A2, KLHL1, OR6C74, DKK4, UNC5A, OR5L1, OR4D2, OR2T33, OR2T6, CDHR1, GJA10, BMP5, OR8H2, INSRR, POSTN, OR4N2, CASQ2, OR2A25, CYP24A1, TAS2R7, OR1E2, OR2B3, SLC45A3, IFNA10, LRRC10, GREM2, OR6N1, CAPN8, TFF3, OR4K5, HOPX, COMP, OR4A5, OR5AN1, KRTAP1-3, OR5AS1, GABRR2, OR13G1, OR2M5, HTR3A, KRTAP13-3, OR13C5, OR4C3, CHST8, MAS1, OR52L1, KRTAP4-2, OR8K1, KIRREL3, OR6B2, KRTAP19-1, KRTAP3-1, KRTAP3-2, KRTAP9-9, OR56A4, PSMA6, OR5B17, TMEM108, OR51A2, P2RX5, OR5T1, OR1A1, OR13C8, OR13C2, GAP43, MFAP5, ADAMTSL1, OR51B4, LCE1F, KCNQ2, SFRP4, OR2AG2, OR2M7, OR51L1, OR5H1, CRLF1, KRTAP21-2, OR8G1, OR6K6, KRTAP19-2, OR10Z1, KRTAP10-1, DNAH11, NPTX2, OR4K1, OR5T2, EDARADD, P116, JPH2, INSC, FN1, ACTBL2, C1QL1, NPFF, OR2A12, BEND6, OR1L8, HBD, OR1J2, TAS2R60, VSIG4, IGF2BP3, CHRNA10, OR5AP2, OR52K1, CYP26B1, FAT3, IL10, TNFRSF11A, GCGR, OR9A2, LCN2, TOP2A, MESP2, CDH22, OR10A5, OR4C46, UCHL1, FGL1, ACTC1, VASP, CIT, CTNNA3, OR52W1, IL5RA, SOSTDC1, TTC8, RADIL, TAS2R8, NTN1, OR52E6, P2RX6, CTNNA2, TTN, OR6K3, MUSTN1, OR11H2, CCR2, P2RY12, CNN1, HRC, PTGS2, DEF8, APOC1, LYZ, GLP1R, NDRG4, CNGA4, APOC2, KRTAP5-1, HADH, SERPINA3, OR52D1, TMEM178A, EFNA4, PIR, HSD17B3, PTGFR, SCRG1, NR6A1, LGI2, AKR1C2, CDH23, ADAMTS2, P2RY1, IGSF11, TSHZ3, PDLIM3, CRYGS, KIF20B, ESR1, ARHGAP22, AGAP2, CYP4F12, SLC26A7, TFCP2L1, RELT, MAP1A, LOXL1, KIF18A, PRICKLE4, JMJD6, ARG2, POU5F1, ROBO1, ALOX5, ANLN, CDK1, SELPLG, GREB1, MYH11, ABCB1, CYP2J2, VAV3, TYMS, SCN1B, MATN3, LAMB3, SRD5A1, SRPX2, SGIP1, GLG1, TPM2, SIX2, SAMHD1

Continued

GO ID	CATEGORY	GO name	Adjusted p value	Negative log10 of adjusted p value	Gene count	Gene
GO:0071944	CC	Cell periphery	1.40E−07	6.853891822	186	HAPLN4, CSNK1G1, IGLL5, PLCH2, SLCO1A2, DMBT1, RGS16, PREX1, LRFN2, NRG3, LRRTM3, GABRA2, NTNG2, GLRA1, DGKG, OR10J3, SLC6A17, OR4F5, SLC18A2, SLC26A9, OR6C74, UNC5A, OR5L1, OR4D2, KCNG3, SLC27A6, OR2T33, CLDN25, OR2T6, ADAM30, CDHR1, GJA10, RASD1, TAAR9, OR8H2, INSRR, POSTN, OR4N2, OR2A25, LY6G6E, TAS2R7, KIF20A, OR1E2, OR2B3, SLC45A3, OR6N1, OR4K5, COMP, OR4A5, OR5AN1, OR5AS1, GABRR2, OR13G1, OR2M5, HTR3A, OR13C5, OR4C3, MAS1, OR52L1, OR8K1, KIRREL3, OR6B2, SLCO5A1, OR56A4, OR5B17, PCDH7, OR51A2, P2RX5, SLC22A9, OR5T1, OR1A1, OR13C8, OR13C2, GAP43, MFAP5, ADAMTSL1, OR51B4, KCNQ2, KCNF1, OR2AG2, CD1E, OR2M7, OR51L1, OR5H1, CRLF1, OR8G1, OR6K6, OR10Z1, KCNH1, OR4K1, OR5T2, SDR16C5, JPH2, INSC, FN1, OR2A12, CAPNS2, YIPF4, OR1L8, OR1J2, TAS2R60, CHRNA10, OR5AP2, MEP1B, OR52K1, FAT3, TNFRSF11A, GCGR, OR9A2, ENTPD3, OXGR1, CDH22, OR10A5, OR4C46, UCHL1, HLA-C, CLEC4D, FGL1, VASP, OR52W1, IL5RA, TTC8, TAS2R8, OLFM4, TSPAN1, GPR141, NTN1, OR52E6, P2RX6, CTNNA2, TTN, OR6K3, OR11H2, CCR2, PRAM1, P2RY12, PTGS2, ITGBL1, GLP1R, NDRG4, KLRK1, CNGA4, SERPINA3, OR52D1, EFNA4, PTGFR, CFB, FCHO1, LRRC7, MMP28, CDH23, ADAMTS2, ATP2C1, P2RY1, IGSF11, TSHZ3, FRMPD1, SELL, ESR1, CYP4F12, RASD2, SLC26A7, LY6G5B, CSF2RA, RELT, LOXL1, KIF18A, B3GNT3, MYO1F, JMJD6, ROBO1, ANLN, SELPLG, ABCB1, DLG2, ADAMTS10, VAV3, SCN1B, LAT, MATN3, LAMB3, SRPX2, SGIP1, SLC7A7, GLG1, SAMHD1
GO:0005886	CC	Plasma membrane	9.39E−07	6.027126436	171	CSNK1G1, IGLL5, PLCH2, SLCO1A2, RGS16, PREX1, LRFN2, NRG3, LRRTM3, GABRA2, NTNG2, GLRA1, DGKG, OR10J3, SLC6A17, OR4F5, SLC18A2, SLC26A9, OR6C74, UNC5A, OR5L1, OR4D2, KCNG3, SLC27A6, OR2T33, CLDN25, OR2T6, ADAM30, CDHR1, GJA10, RASD1, TAAR9, OR8H2, INSRR, OR4N2, OR2A25, LY6G6E, TAS2R7, KIF20A, OR1E2, OR2B3, SLC45A3, OR6N1, OR4K5, OR4A5, OR5AN1, OR5AS1, GABRR2, OR13G1, OR2M5, HTR3A, OR13C5, OR4C3, MAS1, OR52L1, OR8K1, KIRREL3, OR6B2, SLCO5A1, OR56A4, OR5B17, PCDH7, OR51A2, P2RX5, SLC22A9, OR5T1, OR1A1, OR13C8, OR13C2, GAP43, ADAMTSL1, OR51B4, KCNQ2, KCNF1, OR2AG2, CD1E, OR2M7, OR51L1, OR5H1, CRLF1, OR8G1, OR6K6, OR10Z1, KCNH1, OR4K1, OR5T2, SDR16C5, JPH2, INSC, FN1, OR2A12, CAPNS2, YIPF4, OR1L8, OR1J2, TAS2R60, CHRNA10, OR5AP2, MEP1B, OR52K1, FAT3, TNFRSF11A, GCGR, OR9A2, ENTPD3, OXGR1, CDH22, OR10A5, OR4C46, UCHL1, HLA-C, CLEC4D, VASP, OR52W1, IL5RA, TTC8, TAS2R8, OLFM4, TSPAN1, GPR141, OR52E6, P2RX6, CTNNA2, TTN, OR6K3, OR11H2, CCR2, PRAM1, P2RY12, PTGS2, ITGBL1, GLP1R, NDRG4, KLRK1, CNGA4, OR52D1, EFNA4, PTGFR, CFB, FCHO1, LRRC7, CDH23, ATP2C1, P2RY1, IGSF11, TSHZ3, FRMPD1, SELL, ESR1, CYP4F12, RASD2, SLC26A7, LY6G5B, CSF2RA, RELT, KIF18A, B3GNT3, MYO1F, JMJD6, ROBO1, SELPLG, ABCB1, DLG2, VAV3, SCN1B, LAT, SRPX2, SGIP1, SLC7A7, GLG1, SAMHD1
GO:0004888	MF	Transmembranesignaling receptor activity	4.64E−19	18.3338049	83	GABRA2, GLRA1, OR10J3, OR4F5, OR6C74, UNC5A, OR5L1, OR4D2, OR2T33, OR2T6, TAAR9, OR8H2, INSRR, OR4N2, OR2A25, TAS2R7, OR1E2, OR2B3, OR6N1, OR4K5, OR4A5, OR5AN1, OR5AS1, GABRR2, OR13G1, OR2M5, HTR3A, OR13C5, OR4C3, MAS1, OR52L1, OR8K1, OR6B2, OR56A4, OR5B17, OR51A2, P2RX5, OR5T1, OR1A1, OR13C8, OR13C2, OR51B4, OR2AG2, OR2M7, OR51L1, OR5H1, CRLF1, OR8G1, OR6K6, OR10Z1, OR4K1, OR5T2, OR2A12, OR1L8, OR1J2, TAS2R60, CHRNA10, OR5AP2, OR52K1, TNFRSF11A, GCGR, OR9A2, OXGR1, OR10A5, OR4C46, OR52W1, IL5RA, SOSTDC1, TAS2R8, GPR141, OR52E6, P2RX6, OR6K3, OR11H2, CCR2, P2RY12, GLP1R, OR52D1, EFNA4, PTGFR, P2RY1, CSF2RA, ROBO1
GO:0060089	MF	Molecular transducer activity	2.72E-18	17.56616903	88	DMBT1, GABRA2, GLRA1, OR10J3, RXRG, OR4F5, OR6C74, UNC5A, OR5L1, OR4D2, OR2T33, OR2T6, TAAR9, OR8H2, INSRR, OR4N2, OR2A25, TAS2R7, OR1E2, OR2B3, OR6N1, OR4K5, OR4A5, OR5AN1, OR5AS1, GABRR2, OR13G1, OR2M5, HTR3A, OR13C5, OR4C3, MAS1, OR52L1, OR8K1, OR6B2, OR56A4, OR5B17, OR51A2, P2RX5, OR5T1, OR1A1, OR13C8, OR13C2, OR51B4, OR2AG2, OR2M7, OR51L1, OR5H1, CRLF1, OR8G1, OR6K6, OR10Z1, OR4K1, OR5T2, OR2A12, OR1L8, OR1J2, TAS2R60, CHRNA10, OR5AP2, OR52K1, TNFRSF11A, GCGR, OR9A2, OXGR1, OR10A5, OR4C46, OR52W1, IL5RA, SOSTDC1, TAS2R8, GPR141, OR52E6, P2RX6, OR6K3, OR11H2, CCR2, P2RY12, GLP1R, KLRK1, OR52D1, EFNA4, PTGFR, P2RY1, ESR1, CSF2RA, JMJD6, ROBO1

Table 1. The enriched GO terms of the up and down regulated differentially expressed genes.

organism development and nitrogen compound metabolic process. For CC, these up regulated were enriched in membrane-enclosed lumen and nuclear lumen. Moreover, up regulated genes were significantly enriched in protein binding and transcription regulator activity in the MF categories. In addition, the most significantly enriched GO terms for down regulated genes were detection of stimulus and multicellular organismal process (BP), cell periphery and plasma membrane (CC), and transmembrane signaling receptor activity and molecular transducer activity (MF). According to REACTOME pathway enrichment analysis, up regulated genes were significantly enriched in diseases of signal transduction by growth factor receptors and second messengers and formation of the cornified envelope. Down regulated genes were enriched in olfactory signaling pathway and sensory perception.

Construction of the PPI network and module analysis. The PPI network of the DEGs was constructed with 5111 nodes and 9392 edges by using the IntAct database (Fig. 3). A node with a higher node degree, betweenness centrality, stress centrality and closeness centrality consider as a hub genes and are listed in Table 3. The hub genes included MYC, EGFR, LNX1, YBX1, HSP90AA1, ESR1, FN1, TK1, ANLN and SMAD9. To detect significant modules in the PPI network, the PEWCC1 plug-in was used for analysis, and two modules that had the highest degree stood out. GO and pathway enrichment analysis showed that module 1 contained 28

Pathway ID	Pathway name	Adjusted p value	Negative log10 of adjusted p value	Gene count	Gene
Up regulated genes					
REAC:R-HSA-5663202	Diseases of signal transduction by growth factor receptors and second messengers	0.002918856	2.534787284	25	FGA, FGB, FGG, HEYL, HRAS, MYC, IRS1, KIAA1549, STAT1, SYVN1, TCF7L2, DLL4, SOS1, EGFR, PIK3CA, NCSTN, MAML1, MAPK3, TRIM24, ETV6, GSK3A, RNF43, HSP90AA1, GAB1, TNKS
REAC:R-HSA-6809371	Formation of the cornified envelope	0.009712336	2.012676308	12	KRT6A, LCE3D, SPRR3, FLG, SPRR2D, SPRR1B, SPRR1A, KRT16, KRT13, SPRR2E, LCE3E, KLK13
REAC:R-HSA-156827	L13a-mediated translational silencing of Ceruloplasmin expression	0.027095018	1.567110554	10	RPS6, RPL8, RPS28, EIF4B, RPL18, EIF3B, RPL18A, RPS15, RPL39, RPL19
REAC:R-HSA-1643685	Disease	0.027095018	1.567110554	60	CGA, FGA, FGB, FGG, CALCR, ABCB11, MUC21, GCG, ADAMTS8, PTGER4, GPC6, ABCC9, RPS6, SLC29A3, RPL8, HEYL, HRAS, SFTPD, MYC, IRS1, RPS28, MUC6, NUP205, WASF1, PAPSS2, KIAA1549, IL6R, ABCA1, RPL18, STAT1, FMOD, ARPC1A, SYVN1, TCF7L2, DLL4, ELK1, SOS1, PRKACA, EGFR, PIK3CA, NCSTN, MAML1, MAPK3, RPL18A, RPS15, TRIM24, PRKCSH, ETV6, GSK3A, MAOA, RNF43, HSP90AA1, GAB1, S1PR1, RPL39, TNKS, NFKBIA, RPL19, SLC39A4, BSG
REAC:R-HSA-9006934	Signaling by receptor tyrosine kinases	0.03209698	1.493535827	25	IGF2, EGR1, COL6A3, VEGFC, ID3, EGR3, HRAS, IRS1, WASF1, DUSP4, STAT1, ELK1, PTBP1, SOS1, PRKACA, EGFR, PIK3CA, NCSTN, MAPK3, RAB4A, STUB1, HSP90AA1, GAB1, INSR, RALB
REAC:R-HSA-1266738	Developmental biology	0.032172975	1.492508778	45	KRT6A, LCE3D, SPRR3, FLG, SPRR2D, SPRR1B, SPRR1A, DCC, KRT16, ZSCAN10, KRT13, SPRR2E, LCE3E, COL6A3, MPZ, KLK13, RPS6, RPL8, HRAS, MYC, RPS28, IL6R, PBX1, RPL18, ARPC1A, HELZ2, SOS1, PRKACA, EGFR, PIK3CA, MED13L, NCSTN, MAML1, MAPK3, RPL18A, ACVR2B, RPS15, HSP90AA1, GAB1, RPL39, MED25, CASC3, SIAH2, RNPS1, RPL19
Down regulated genes					
REAC:R-HSA-381753	Olfactory signaling pathway	4.32E−23	22.36427935	54	OR10J3, OR4F5, OR6C74, OR5L1, OR4D2, OR2T33, OR2T6, OR8H2, OR4N2, OR2A25, OR1E2, OR2B3, OR6N1, OR4K5, OR4A5, OR5AN1, OR5AS1, OR13G1, OR2M5, OR13C5, OR4C3, OR52L1, OR8K1, OR6B2, OR56A4, OR5B17, OR51A2, OR5T1, OR1A1, OR13C8, OR13C2, OR51B4, OR2AG2, OR2M7, OR51L1, OR5H1, OR8G1, OR6K6, OR10Z1, OR4K1, OR5T2, OR2A12, OR1L8, OR1J2, OR5AP2, OR52K1, OR9A2, OR10A5, OR4C46, OR52W1, OR52E6, OR6K3, OR11H2, OR52D1
REAC:R-HSA-9709957	Sensory perception	4.85E−21	20.31389969	57	OR10J3, OR4F5, OR6C74, OR5L1, OR4D2, OR2T33, OR2T6, OR8H2, OR4N2, OR2A25, OR1E2, OR2B3, OR6N1, OR4K5, OR4A5, OR5AN1, OR5AS1, OR13G1, OR2M5, OR13C5, OR4C3, OR52L1, OR8K1, OR6B2, OR56A4, OR5B17, OR51A2, OR5T1, OR1A1, OR13C8, OR13C2, OR51B4, OR2AG2, OR2M7, OR51L1, OR5H1, OR8G1, OR6K6, OR10Z1, OR4K1, OR5T2, OR2A12, OR1L8, RDH16, OR1J2, OR5AP2, OR52K1, OR9A2, OR10A5, OR4C46, OR52W1, OR52E6, OR6K3, BCO2, OR11H2, APOC2, OR52D1
Continued					

Pathway ID	Pathway name	Adjusted p value	Negative log10 of adjusted p value	Gene count	Gene
REAC:R-HSA-418555	G alpha (s) signalling events	6.29E−20	19.20156126	58	IAPP, ADCYAP1, OR10J3, OR4F5, OR6C74, OR5L1, OR4D2, OR2T33, OR2T6, TAAR9, OR8H2, OR4N2, OR2A25, OR1E2, OR2B3, OR6N1, OR4K5, OR4A5, OR5AN1, OR5AS1, OR13G1, OR2M5, OR13C5, OR4C3, OR52L1, OR8K1, OR6B2, OR56A4, OR5B17, OR51A2, OR5T1, OR1A1, OR13C8, OR13C2, OR51B4, OR2AG2, OR2M7, OR51L1, OR5H1, OR8G1, OR6K6, OR10Z1, OR4K1, OR5T2, OR2A12, OR1L8, OR1J2, OR5AP2, OR52K1, OR9A2, OR10A5, OR4C46, OR52W1, OR52E6, OR6K3, OR11H2, GLP1R, OR52D1
REAC:R-HSA-388396	GPCR downstream signalling	9.32E−15	14.0308131	76	IAPP, ADCYAP1, RGS16, PREX1, DGKG, OR10J3, OR4F5, OR6C74, OR5L1, OR4D2, ARHGEF35, OR2T33, OR2T6, TAAR9, OR8H2, OR4N2, OR2A25, TAS2R7, OR1E2, OR2B3, OR6N1, OR4K5, OR4A5, OR5AN1, OR5AS1, OR13G1, OR2M5, OR13C5, OR4C3, OR52L1, OR8K1, OR6B2, OR56A4, OR5B17, OR51A2, OR5T1, OR1A1, OR13C8, OR13C2, OR51B4, OR2AG2, OR2M7, OR51L1, OR5H1, OR8G1, OR6K6, OR10Z1, OR4K1, OR5T2, NPFF, OR2A12, OR1L8, RDH16, OR1J2, TAS2R60, OR5AP2, OR52K1, OR9A2, OXGR1, OR10A5, OR4C46, OR52W1, TAS2R8, OR52E6, OR6K3, BCO2, OR11H2, CCR2, P2RY12, GLP1R, APOC2, OR52D1, PTGFR, P2RY1, PDE1C, VAV3
REAC:R-HSA-372790	Signaling by GPCR	2.45E−13	12.61114695	76	IAPP, ADCYAP1, RGS16, PREX1, DGKG, OR10J3, OR4F5, OR6C74, OR5L1, OR4D2, ARHGEF35, OR2T33, OR2T6, TAAR9, OR8H2, OR4N2, OR2A25, TAS2R7, OR1E2, OR2B3, OR6N1, OR4K5, OR4A5, OR5AN1, OR5AS1, OR13G1, OR2M5, OR13C5, OR4C3, OR52L1, OR8K1, OR6B2, OR56A4, OR5B17, OR51A2, OR5T1, OR1A1, OR13C8, OR13C2, OR51B4, OR2AG2, OR2M7, OR51L1, OR5H1, OR8G1, OR6K6, OR10Z1, OR4K1, OR5T2, NPFF, OR2A12, OR1L8, RDH16, OR1J2, TAS2R60, OR5AP2, OR52K1, OR9A2, OXGR1, OR10A5, OR4C46, OR52W1, TAS2R8, OR52E6, OR6K3, BCO2, OR11H2, CCR2, P2RY12, GLP1R, APOC2, OR52D1, PTGFR, P2RY1, PDE1C, VAV3
REAC:R-HSA-162582	Signal transduction	7.38146E−05	4.131857963	105	IAPP, ADCYAP1, RGS16, PREX1, NRG3, DLK1, DGKG, OR10J3, RXRG, OR4F5, OR6C74, DKK4, OR5L1, OR4D2, ARHGEF35, OR2T33, OR2T6, TAAR9, OR8H2, OR4N2, OR2A25, TAS2R7, OR1E2, OR2B3, GREM2, OR6N1, TFF3, OR4K5, OR4A5, OR5AN1, OR5AS1, OR13G1, OR2M5, OR13C5, OR4C3, OR52L1, OR8K1, OR6B2, OR56A4, PSMA6, DLGAP5, OR5B17, OR51A2, OR5T1, OR1A1, OR13C8, OR13C2, OR51B4, OR2AG2, OR2M7, OR51L1, OR5H1, OR8G1, OR6K6, OR10Z1, OR4K1, OR5T2, SDR16C5, FN1, NPFF, OR2A12, OR1L8, RDH16, OR1J2, TAS2R60, OR5AP2, OR52K1, CYP26B1, OR9A2, OXGR1, OR10A5, SPC24, OR4C46, CIT, OR52W1, IL5RA, TAS2R8, OR52E6, OR6K3, BCO2, OR11H2, CCR2, P2RY12, APOC1, GLP1R, APOC2, OR52D1, SMAD9, PTGFR, BUB1B, P2RY1, ARHGAP20, NEDD8, ESR1, ARHGAP22, CSF2RA, KIF18A, ARHGAP9, CDK1, GREB1, MYH11, PDE1C, DLG2, VAV3, LAMB3

Table 2. The enriched pathway terms of the up and down regulated differentially expressed genes.

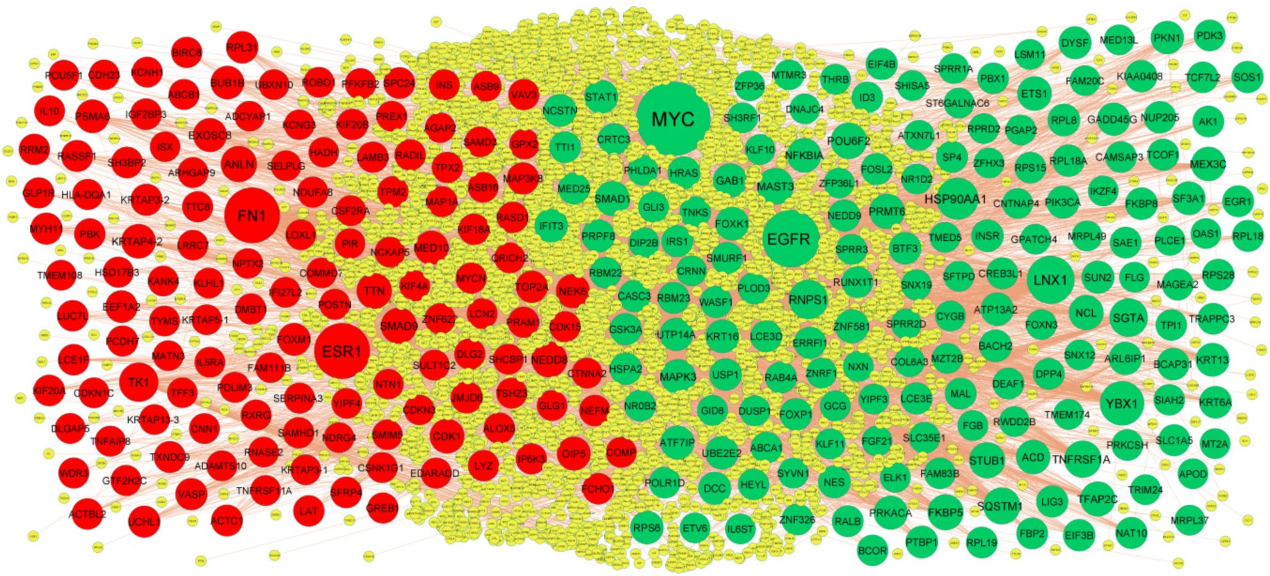

Figure 3. PPI network of DEGs. The PPI network of DEGs was constructed using Cytoscap. Up regulated genes are marked in green; down regulated genes are marked in red.

nodes and 63 edges (Fig. 4A), which were associated with diseases of signal transduction by growth factor receptors and second messengers, disease, nitrogen compound metabolic process and membrane-enclosed lumen, while module 2 had 14 nodes and 30 edges (Fig. 4B), which were mainly associated with signal transduction, multicellular organismal process and detection of stimulus.

MiRNA-hub gene regulatory network construction. The network of miRNAs and predicted targets (hub genes) is presented in Table 4. Based on the miRNAs, a miRNA -hub gene regulatory network was constructed with 2568 nodes (miRNA: 2259; hub gene: 309) and 16,618 interaction pairs (Fig. 5). Notably, MYC targeted 194 miRNAs, including hsa-mir-4677-3p; HSP90AA1 targeted 188 miRNAs, including hsa-mir-3125; FKBP5 targeted 116 miRNAs, including hsa-mir-4779; RNPS1 targeted 109 miRNAs, including hsa-mir-548az-3p; SQSTM1 targeted 108 miRNAs, including hsa-mir-106a-5p; ANLN targeted 127 miRNAs, including hsa-mir-664a-3p; CDK1 targeted 109 miRNAs, including hsa-mir-5688;FN1 targeted 105 miRNAs, including hsa-mir-199b-3p;ESR1 targeted 98 miRNAs, including hsa-mir-206; TK1 targeted 80 miRNAs, including hsa-mir-6512-3p.

TF-hub gene regulatory network construction. The network of TFs and predicted targets (hub genes) is presented in Table 4. Based on the TFs, a TF -hub gene regulatory network was constructed with 899 nodes (TF: 604; hub gene: 295) and 3542 interaction pairs (Fig. 6). Notably, MAPK3 targeted 48 TFs, including JUND; HSP90AA1 targeted 35 TFs, including HSF2; SQSTM1 targeted 34 TFs, including SMAD4; STUB1 targeted 31 TFs, including ATF6; EGFR targeted 27 TFs, including ELF3; ESR1 targeted 126 TFs, including ELF3; SMAD9 targeted 38 TFs, including ELF3; CDK1 targeted 36 TFs, including ELF3; FN1 targeted 25 TFs, including ELF3; NEK6 targeted 16 TFs, including ELF3.

Validation of hub genes by receiver operating characteristic curve (ROC) analysis. As these 10 hub genes are prominently expressed in T1DM, we performed a ROC curve analysis to evaluate their sensitivity and specificity for the diagnosis of T1DM. As shown in Fig. 7, MYC, EGFR, LNX1, YBX1, HSP90AA1, ESR1, FN1, TK1, ANLN and SMAD9 achieved an AUC value of > 0.9, demonstrating that these genes have high sensitivity and specificity for T1DM diagnosis. The results suggested that MYC, EGFR, LNX1, YBX1, HSP90AA1, ESR1, FN1, TK1, ANLN and SMAD9 can be used as biomarkers for the diagnosis of T1DM.

Discussion

T1DM is the common forms of chronic autoimmune diabetes that affect an individual's quality of childhood life[42]. However, the potential causes of T1DM remain uncertain. Understanding the underlying molecular pathogenesis of T1DM is of key importance for diagnosis, prognosis and identifying drug targets. As NGS data can provide information regarding the expression levels of thousands of genes in the human genome simultaneously, this methodology has been widely used to predict the potential diagnostic and therapeutic targets for T1DM. In the present investigation, we analyzed the NGS dataset GSE162689, which includes 27 T1DM samples and 32 normal control samples. We identified 477 up regulated and 475 down regulated genes between T1DM samples and normal control samples using DESeq2 package in R language software. FGA (fibrinogen alpha chain)[43] and FGB (fibrinogen beta chain)[44] levels are correlated with disease severity in patients with cardiovascular disease, but these genes might provide new targets for the development of drugs to treat T1DM. IGF2[45], IAPP (islet amyloid

Regulation	Node	Degree	Betweenness	Stress	Closeness
Up	MYC	769	0.24506	1.04E + 08	0.402932
Up	EGFR	469	0.138032	61,812,344	0.381322
Up	LNX1	301	0.098028	35,639,540	0.344753
Up	YBX1	242	0.052423	15,440,248	0.370488
Up	HSP90AA1	198	0.042012	18,645,766	0.349323
Up	RNPS1	148	0.029398	16,186,898	0.324119
Up	SGTA	139	0.039126	11,319,544	0.315439
Up	TNFRSF1A	116	0.016842	8,191,032	0.328598
Up	SQSTM1	112	0.025913	6,213,766	0.344335
Up	MAST3	105	0.022	12,287,012	0.305669
Up	POU6F2	99	0.028224	4,939,174	0.317338
Up	STUB1	95	0.01869	5,557,470	0.333856
Up	FKBP5	94	0.015263	3,991,284	0.329764
Up	PRMT6	82	0.023047	4,016,020	0.301486
Up	MAPK3	78	0.01798	4,710,364	0.312259
Up	SMAD1	77	0.014129	5,216,492	0.309237
Up	TFAP2C	77	0.020062	3,309,460	0.333573
Up	NCL	73	0.015947	5,344,646	0.374917
Up	ETS1	69	0.014065	3,895,426	0.310987
Up	MEX3C	68	0.003769	2,594,352	0.310439
Up	ACD	66	0.014094	3,525,238	0.307138
Up	NFKBIA	66	0.008138	4,939,524	0.310854
Up	GAB1	61	0.005759	2,357,788	0.296365
Up	ZNF581	58	0.008074	2,392,056	0.303509
Up	PRKACA	58	0.012141	2,683,394	0.312833
Up	KRT13	56	0.009539	2,356,276	0.31577
Up	SF3A1	54	0.005297	3,631,052	0.304231
Up	STAT1	54	0.010129	1,749,810	0.330531
Up	ATF7IP	54	0.011319	2,610,676	0.297746
Up	FOXK1	52	0.010322	2,431,366	0.309968
Up	KRT16	52	0.009137	2,768,286	0.302646
Up	RPS6	50	0.005709	1,809,230	0.323503
Up	IFIT3	48	0.004333	1,419,676	0.307396
Up	UBE2E2	48	0.009384	2,778,786	0.289714
Up	PKN1	47	0.007325	2,119,206	0.29714
Up	ARL6IP1	46	0.011853	5,167,578	0.284047
Up	UTP14A	45	0.00788	1,716,012	0.322239
Up	PRPF8	44	0.006824	1,731,078	0.329977
Up	GADD45G	44	0.007648	1,727,574	0.29879
Up	ATP13A2	43	0.011364	3,235,048	0.28605
Up	HRAS	42	0.006113	1,934,688	0.306916
Up	DCC	42	0.005613	2,081,812	0.292265
Up	SUN2	42	0.004561	2,137,880	0.299806
Up	DYSF	41	0.007116	2,286,238	0.293962
Up	NCSTN	40	0.007729	5,776,106	0.274308
Up	RPL8	37	0.004561	1,421,422	0.324922
Up	BACH2	37	0.008838	2,796,552	0.273369
Up	PIK3CA	37	0.005768	1,280,756	0.304576
Up	PTBP1	36	0.003339	1,190,818	0.333507
Up	FKBP8	35	0.00586	1,371,274	0.3223
Up	NES	35	0.007013	1,126,640	0.295338
Up	KRT6A	34	0.005784	1,381,296	0.320281
Up	NUP205	33	0.005495	1,090,580	0.323442
Up	FOXP1	33	0.006278	1,144,548	0.31992
Up	INSR	33	0.003132	1,562,024	0.279757
Up	BCAP31	32	0.00482	1,838,970	0.292131
Continued					

Regulation	Node	Degree	Betweenness	Stress	Closeness
Up	BTF3	31	0.00454	1,476,600	0.290636
Up	RPL18A	31	0.002498	754,566	0.318306
Up	KIAA0408	30	0.00425	1,221,042	0.302575
Up	USP1	30	0.004591	2,441,058	0.280879
Up	EIF3B	29	0.003846	916,674	0.315848
Up	HSPA2	28	0.002862	684,442	0.313947
Up	RPS28	28	0.002873	1,278,818	0.301718
Up	SOS1	28	0.002513	879,664	0.284205
Up	ERRFI1	26	0.002199	611,152	0.311214
Up	LCE3E	26	0.001327	524,110	0.25448
Up	GSK3A	26	0.004252	1,655,588	0.292867
Up	NAT10	26	0.001696	666,842	0.325191
Up	LIG3	26	0.00228	725,644	0.294691
Up	RPL18	25	9.73E−04	477,540	0.322646
Up	SLC1A5	25	0.004674	807,018	0.306677
Up	EIF4B	25	0.00188	620,280	0.295594
Up	NEDD9	24	0.003127	549,922	0.289271
Up	CASC3	23	0.002491	601,190	0.302503
Up	FOSL2	23	0.003682	831,006	0.310911
Up	SMURF1	22	0.002704	664,080	0.284142
Up	PLOD3	22	0.003554	1,082,282	0.335808
Up	TCOF1	22	0.00218	501,286	0.314295
Up	ZNF326	22	0.001349	640,724	0.29001
Up	SP4	22	0.003993	853,624	0.26749
Up	EGR1	21	0.002422	466,912	0.302056
Up	MAGEA2	21	0.004402	1,011,862	0.293759
Up	CREB3L1	21	0.006704	4,786,040	0.227129
Up	WASF1	20	0.003044	1,067,564	0.274868
Up	IRS1	20	0.001568	411,892	0.309837
Up	CRTC3	20	0.002135	967,284	0.279558
Up	FBP2	20	9.48E−04	423,694	0.288846
Up	MED25	20	0.001218	294,794	0.275609
Up	LCE3D	20	4.82E−04	304,904	0.263329
Up	DEAF1	19	0.002531	618,844	0.3017
Up	PDK3	19	0.003011	604,606	0.307526
Up	RPL19	19	6.37E−04	392,064	0.319241
Up	ABCA1	19	0.004473	1,062,228	0.298441
Up	SAE1	19	0.003167	702,666	0.299157
Up	MAL	19	0.004533	1,470,896	0.264227
Up	RAB4A	19	0.003857	747,204	0.292398
Up	RALB	19	0.001738	1,634,506	0.255536
Up	TRAPPC3	19	0.005096	1,890,182	0.252046
Up	DPP4	19	0.00527	1,619,646	0.234023
Up	PRKCSH	18	0.002123	375,070	0.316043
Up	RBM22	18	0.002051	950,490	0.283386
Up	CAMSAP3	18	0.002085	1,031,300	0.274014
Up	AK1	18	0.002632	1,174,620	0.257986
Up	TTI1	17	0.001947	994,560	0.275505
Up	RUNX1T1	17	0.002454	1,455,104	0.275046
Up	RPS15	16	0.00225	468,552	0.316395
Up	NR0B2	16	0.002709	597,146	0.313581
Up	POLR1D	16	0.001752	656,232	0.282369
Up	FAM83B	16	8.49E−04	301,500	0.277314
Up	PBX1	16	0.001944	703,560	0.258718
Up	TCF7L2	15	0.001345	373,312	0.28326
Up	BCOR	15	0.002336	806,128	0.273164
Continued					

Regulation	Node	Degree	Betweenness	Stress	Closeness
Up	ID3	15	0.002818	819,716	0.269962
Up	SLC35E1	15	0.003323	1,409,720	0.24654
Up	TPI1	14	0.002071	457,522	0.314391
Up	SIAH2	14	0.001994	845,214	0.269677
Up	TNKS	14	0.002475	650,184	0.251959
Up	RBM23	14	2.87E−04	166,572	0.276758
Up	HEYL	14	0.002211	402,860	0.280864
Up	MRPL37	2	1.61E−04	51,382	0.28108
Up	GID8	2	4.01E−05	6218	0.246921
Up	DIP2B	2	0	0	0.291299
Up	SH3RF1	2	2.53E−04	99,400	0.287919
Up	ZFP36L1	2	9.45E−05	13,940	0.255792
Up	GCG	2	1.27E−04	41,870	0.209131
Up	YIPF3	2	7.28E−05	18,416	0.211048
Up	FGB	1	0	0	0.254404
Up	FAM20C	1	0	0	0.254404
Up	GLI3	1	0	0	0.236207
Up	NXN	1	0	0	0.215614
Up	PHLDA1	1	0	0	0.276071
Up	SPRR1A	1	0	0	0.276071
Up	DNAJC4	1	0	0	0.276071
Up	MRPL49	1	0	0	0.270347
Up	COL6A3	1	0	0	0.22719
Up	MZT2B	1	0	0	0.287223
Up	ZFHX3	1	0	0	0.287223
Up	SNX19	1	0	0	0.287223
Up	KLF10	1	0	0	0.287223
Up	ST6GALNAC6	1	0	0	0.287223
Up	RPRD2	1	0	0	0.287223
Up	ETV6	1	0	0	0.287223
Up	SYVN1	1	0	0	0.273764
Up	SPRR2D	1	0	0	0.229084
Up	FGF21	1	0	0	0.239809
Up	TMEM174	1	0	0	0.239809
Up	CYGB	1	0	0	0.222435
Up	CRNN	1	0	0	0.256151
Up	PLCE1	1	0	0	0.258901
Up	SFTPD	1	0	0	0.201125
Up	TRIM24	1	0	0	0.273179
Up	APOD	1	0	0	0.273179
Up	THRB	1	0	0	0.21607
Up	IKZF4	1	0	0	0.23715
Up	SPRR3	1	0	0	0.23715
Up	CNTNAP4	1	0	0	0.23412
Up	ZNRF1	1	0	0	0.224644
Up	ATXN7L1	1	0	0	0.211048
Up	FLG	1	0	0	0.219296
Up	MT2A	1	0	0	0.250147
Up	SHISA5	1	0	0	0.250147
Up	RWDD2B	1	0	0	0.230063
Up	OAS1	1	0	0	0.231658
Up	TMED5	1	0	0	0.231658
Up	NR1D2	1	0	0	0.231658
Up	GPATCH4	1	0	0	0.228011
Up	KLF11	1	0	0	0.217829
Up	ZFP36	1	0	0	0.239696
Continued					

Regulation	Node	Degree	Betweenness	Stress	Closeness
Up	MTMR3	1	0	0	0.239696
Up	FOXN3	1	0	0	0.239696
Up	PGAP2	1	0	0	0.221817
Up	ELK1	1	0	0	0.237967
Up	DUSP1	1	0	0	0.237967
Up	IL6ST	1	0	0	0.248433
Up	SNX12	1	0	0	0.221222
Up	LSM11	1	0	0	0.237183
Up	MED13L	1	0	0	0.232501
Down	ESR1	448	0.115717	68,567,806	0.375827
Down	FN1	445	0.130416	47,618,446	0.393806
Down	TK1	155	0.044276	10,622,930	0.341187
Down	ANLN	102	0.019831	5,950,428	0.327945
Down	SMAD9	99	0.023512	10,495,428	0.31337
Down	NEDD8	94	0.013216	4,708,022	0.323626
Down	TTN	88	0.021791	4,877,390	0.354606
Down	CDK1	76	0.019122	4,123,802	0.343387
Down	KRTAP4-2	73	0.019925	3,654,538	0.300106
Down	MED10	65	0.012717	3,973,710	0.302915
Down	EXOSC8	61	0.015702	2,371,472	0.315244
Down	NEK6	61	0.009473	2,973,110	0.31289
Down	OIP5	60	0.013758	3,810,166	0.30688
Down	PSMA6	57	0.012284	2,937,164	0.324778
Down	BUB1B	54	0.010813	5,323,030	0.298111
Down	FOXM1	43	0.007242	2,131,654	0.300317
Down	RPL31	35	0.003717	1,156,016	0.323013
Down	EEF1A2	33	0.002074	927,396	0.307212
Down	JMJD6	31	0.006976	4,154,054	0.261751
Down	VASP	30	0.005691	1,017,020	0.316768
Down	MAP3K8	30	0.001715	773,154	0.310458
Down	UCHL1	28	0.003224	905,164	0.308808
Down	TOP2A	28	0.0032	1,042,178	0.328788
Down	MYH11	28	0.003406	1,173,838	0.305103
Down	RASSF1	27	0.004112	1,253,252	0.299175
Down	KRTAP3-2	27	0.004532	1,398,432	0.265421
Down	TXNDC9	26	0.004126	1,143,166	0.278477
Down	ACTC1	24	0.004063	1,053,202	0.329594
Down	SPC24	23	0.002762	801,496	0.268982
Down	SH3BP2	21	0.001863	813,564	0.277887
Down	IGF2BP3	20	0.001318	388,432	0.332401
Down	KIF20A	20	0.004794	850,452	0.262706
Down	SFRP4	20	0.001565	724,830	0.277404
Down	KIF20B	18	0.003465	529,620	0.306935
Down	RASD1	18	0.001969	611,526	0.282869
Down	NEFM	18	0.002405	500,776	0.29515
Down	RADIL	18	0.001925	718,708	0.28187
Down	LCE1F	18	5.31E−04	1,078,996	0.215551
Down	LUC7L	17	0.001779	331,232	0.297175
Down	LYZ	17	0.002823	462,382	0.311441
Down	PFKFB2	17	0.002624	984,686	0.285029
Down	ACTBL2	17	5.95E−04	248,094	0.310647
Down	FCHO1	17	0.002083	725,112	0.267588
Down	KIF18A	17	0.002914	1,632,588	0.264802
Down	SAMHD1	16	0.002408	964,652	0.269962
Down	LAT	15	0.002067	607,316	0.301593
Down	PBK	15	0.002668	669,380	0.294912
Continued					

Regulation	Node	Degree	Betweenness	Stress	Closeness
Down	TPX2	15	9.04E−04	407,858	0.293506
Down	RRM2	15	0.002347	419,566	0.272147
Down	LAMB3	15	0.002279	1,460,718	0.265531
Down	ALOX5	15	0.003126	496,364	0.267099
Down	TPM2	15	4.76E−04	162,954	0.290092
Down	IP6K3	14	0.001497	346,042	0.275387
Down	VAV3	14	0.001429	470,180	0.297573
Down	NDUFA8	13	0.00167	479,156	0.290455
Down	BIRC8	13	0.002152	927,372	0.24679
Down	DLG2	13	0.002105	767,688	0.273896
Down	MYCN	12	1.11E−04	41,976	0.304939
Down	PRAM1	12	0.001039	343,780	0.260883
Down	PCDH7	12	0.001704	788,890	0.266375
Down	EDARADD	11	0.001215	325,252	0.268544
Down	GREB1	11	9.15E−04	206,196	0.268968
Down	ZNF622	11	8.30E−04	730,808	0.269663
Down	RXRG	11	0.002054	800,986	0.250012
Down	GLP1R	11	3.87E−04	306,068	0.257778
Down	TTC8	11	0.003532	958,578	0.227362
Down	SERPINA3	10	0.002011	543,412	0.243151
Down	CDK15	10	2.37E−04	85,694	0.294623
Down	HLA-DQA1	10	0.001488	682,934	0.249878
Down	HSD17B3	10	1.13E−04	75,794	0.26087
Down	TSHZ3	10	0.001111	304,690	0.256253
Down	MAP1A	9	8.61E−04	207,068	0.312393
Down	CSNK1G1	9	0.001614	637,430	0.248529
Down	GTF2H2C	9	0.001734	341,202	0.245876
Down	PDLIM3	9	0.001957	559,870	0.239831
Down	WDR3	9	6.45E−04	234,640	0.274455
Down	TNFAIP8	9	9.44E−04	850,962	0.230957
Down	ADAMTS10	8	9.45E−04	260,474	0.258443
Down	ABCB1	8	9.74E−04	146,904	0.3
Down	QRICH2	8	0.001291	295,070	0.261336
Down	INS	8	4.75E−04	194,074	0.248216
Down	COMP	8	0.001207	326,670	0.231995
Down	SHCBP1	7	4.46E−04	233,846	0.256678
Down	DLGAP5	7	1.46E−04	74,806	0.290108
Down	ARHGAP9	7	3.62E−04	66,924	0.28522
Down	KCNH1	7	3.41E−04	213,892	0.253094
Down	KLHL1	6	1.15E−04	30,788	0.283638
Down	LCN2	6	4.47E−04	83,350	0.256575
Down	TYMS	6	4.58E−04	134,624	0.25317
Down	CDKN1C	6	4.20E−04	155,814	0.26589
Down	DMBT1	6	0.001176	361,022	0.251748
Down	SULT1C2	6	4.34E−04	98,520	0.244289
Down	IL10	6	8.05E−04	231,670	0.245675
Down	SAMD3	6	6.69E−04	135,970	0.268713
Down	NCKAP5	6	4.03E−05	22,814	0.2639
Down	CNN1	6	2.65E−04	64,314	0.23624
Down	PREX1	6	8.35E−04	387,030	0.254975
Down	CTNNA2	5	5.71E−04	182,504	0.281204
Down	POU5F1	5	7.40E−04	107,680	0.274839
Down	POSTN	5	5.96E−04	207,158	0.228766
Down	CSF2RA	5	8.10E−04	258,390	0.252907
Down	MATN3	5	1.69E−04	28,890	0.235848
Down	ASB9	5	5.76E−04	238,362	0.238055
Continued					

Regulation	Node	Degree	Betweenness	Stress	Closeness
Down	KRTAP5-1	5	0.001174	179,682	0.190051
Down	IL5RA	5	0.001176	281,872	0.257441
Down	KANK4	5	7.94E−04	141,232	0.240633
Down	ASB16	5	2.41E−05	16,592	0.266028
Down	KIF4A	5	4.60E−05	13,994	0.259374
Down	ROBO1	5	4.93E−04	116,624	0.246421
Down	TNFRSF11A	4	4.04E−04	116,804	0.251934
Down	KRTAP3-1	4	2.89E−05	20,452	0.252494
Down	UBXN10	4	5.63E−04	69,202	0.248047
Down	GLG1	4	4.17E−04	62,018	0.265572
Down	LOXL1	4	4.78E−04	74,588	0.250404
Down	COMMD7	4	4.03E−04	180,366	0.233127
Down	SELPLG	4	8.09E−04	244,340	0.221136
Down	YIPF4	4	4.79E−05	15,522	0.197986
Down	TMEM108	4	2.77E−05	10,972	0.243081
Down	KRTAP13-3	3	3.50E−07	422	0.210396
Down	LRRC7	3	7.82E−04	166,682	0.180159
Down	GPX2	2	0	0	0.299578
Down	CDH23	1	0	0	0.215614
Down	ISX	1	0	0	0.240905
Down	NPTX2	1	0	0	0.287223
Down	KCNG3	1	0	0	0.287223
Down	SMIM5	1	0	0	0.239809
Down	TFF3	1	0	0	0.239809
Down	FAM111B	1	0	0	0.222435
Down	CDKN3	1	0	0	0.255626
Down	IFI27L2	1	0	0	0.250147
Down	NTN1	1	0	0	0.226175
Down	AGAP2	1	0	0	0.218611
Down	PIR	1	0	0	0.238611
Down	RNASE2	1	0	0	0.215016
Down	ADCYAP1	1	0	0	0.189649
Down	HADH	1	0	0	0.248433
Down	NDRG4	1	0	0	0.221222

Table 3. Topology table for up and down regulated genes.

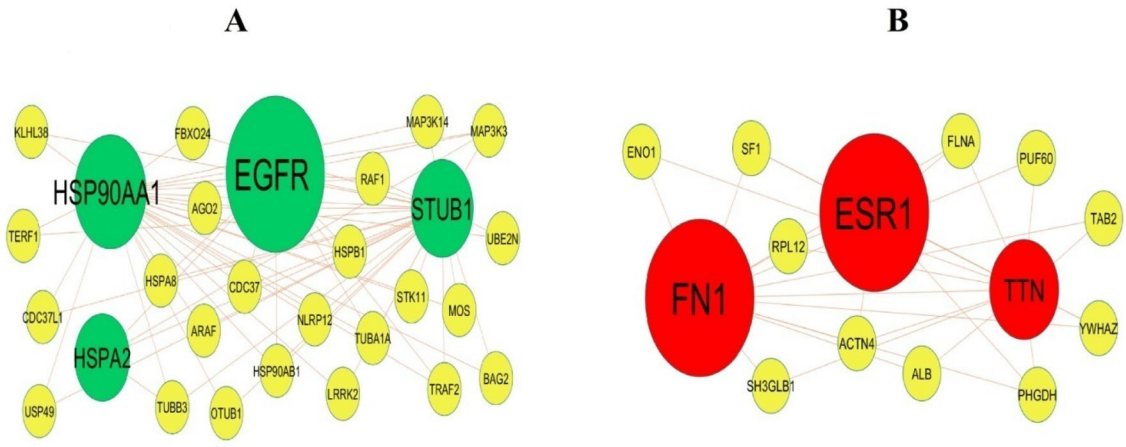

Figure 4. Modules of isolated form PPI of DEGs. (**A**) The most significant module was obtained from PPI network with 28 nodes and 63 edges for up regulated genes (**B**) The most significant module was obtained from PPI network with 14 nodes and 30 edges for down regulated genes. Up regulated genes are marked in green; down regulated genes are marked in red.

Regulation	Target genes	Degree	MicroRNA	Regulation	Target genes	Degree	TF
Up	MYC	194	hsa-mir-4677-3p	Up	MAPK3	48	JUND
Up	HSP90AA1	188	hsa-mir-3125	Up	HSP90AA1	35	HSF2
Up	FKBP5	116	hsa-mir-4779	Up	SQSTM1	34	SMAD4
Up	RNPS1	109	hsa-mir-548az-3p	Up	STUB1	31	ATF6
Up	SQSTM1	108	hsa-mir-106a-5p	Up	EGFR	27	ELF3
Up	EGFR	83	hsa-mir-219a-5p	Up	YBX1	24	TFAP2A
Up	MAST3	76	hsa-mir-129-2-3p	Up	LNX1	21	MAX
Up	YBX1	48	hsa-mir-1537-3p	Up	FKBP5	20	PGR
Up	PRMT6	43	hsa-mir-4330	Up	PRMT6	9	YY1
Up	MAPK3	33	hsa-mir-3158-3p	Up	SGTA	7	MXI1
Up	SGTA	24	hsa-mir-421	Up	POU6F2	7	ALX1
Up	TNFRSF1A	22	hsa-mir-548an	Up	RNPS1	7	STAT3
Up	STUB1	16	hsa-mir-942-5p	Up	TNFRSF1A	6	EP300
Up	POU6F2	15	hsa-mir-7850-5p	Up	MAST3	1	NFYA
Down	ANLN	127	hsa-mir-664a-3p	Down	ESR1	126	FOXF2
Down	CDK1	109	hsa-mir-5688	Down	SMAD9	38	XAB2
Down	FN1	105	hsa-mir-199b-3p	Down	CDK1	36	KHDRBS1
Down	ESR1	98	hsa-mir-206	Down	FN1	25	RELA
Down	TK1	80	hsa-mir-6512-3p	Down	NEK6	16	SRY
Down	OIP5	62	hsa-mir-767-5p	Down	TK1	11	DRAP1
Down	SMAD9	58	hsa-mir-3689a-3p	Down	NEDD8	10	PARP1
Down	MED10	41	hsa-mir-647	Down	TTN	10	FOXD3
Down	NEK6	34	hsa-mir-4485-3p	Down	ANLN	9	JUN
Down	BUB1B	32	hsa-mir-449b-5p	Down	BUB1B	9	MYB
Down	TTN	31	hsa-mir-181c-5p	Down	MED10	6	KDM4B
Down	NEDD8	26	hsa-mir-583	Down	PSMA6	6	EBF1
Down	PSMA6	17	hsa-mir-539-5p	Down	OIP5	5	GATA2
Down	EXOSC8	17	hsa-mir-191-5p	Down	KRTAP4-2	1	TBP

Table 4. miRNA-target gene and TF-target gene interaction.

Figure 5. MiRNA—hub gene regulatory network. The chocolate color diamond nodes represent the key miRNAs; up regulated genes are marked in green; down regulated genes are marked in red.

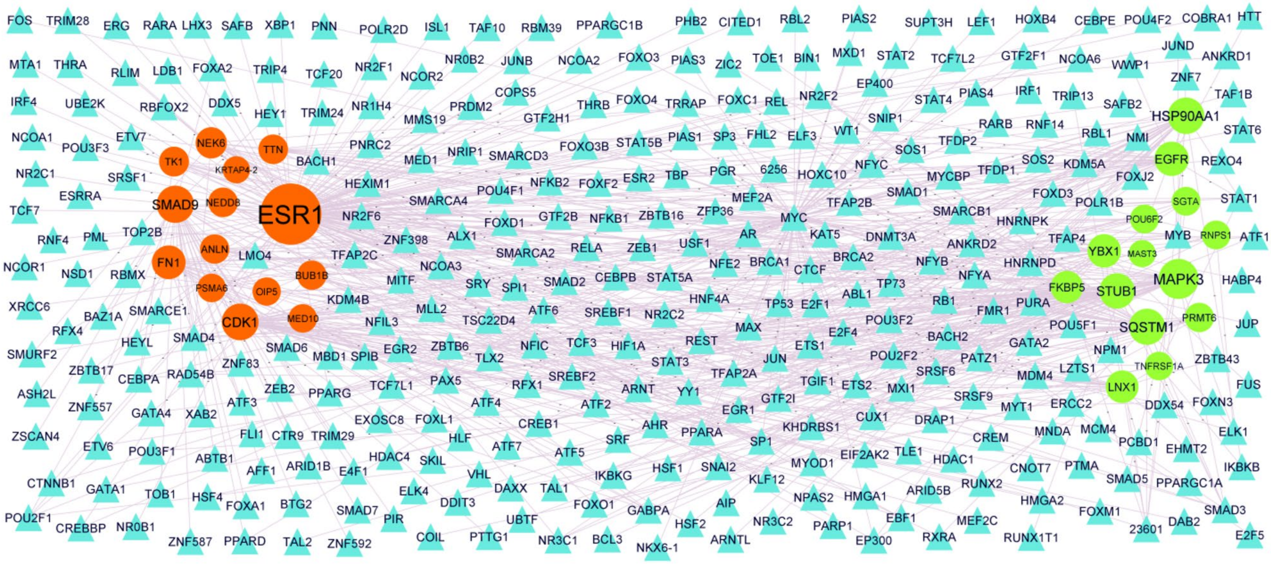

Figure 6. TF—hub gene regulatory network. The blue color triangle nodes represent the key TFs; up regulated genes are marked in green; down regulated genes are marked in red.

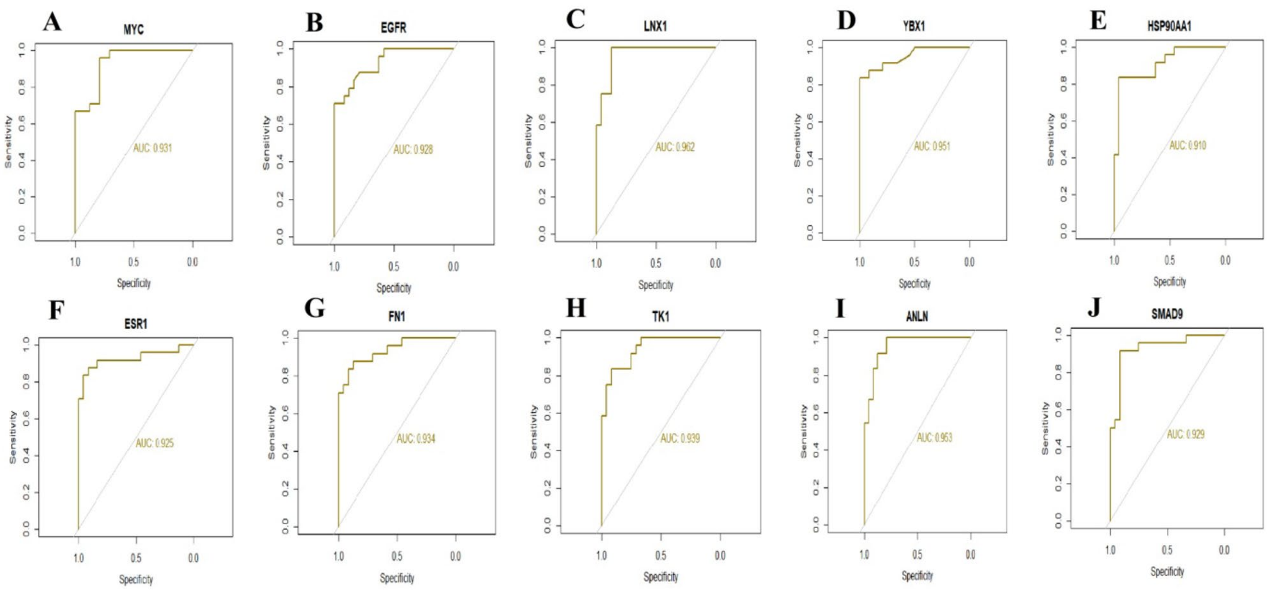

Figure 7. ROC curve validated the sensitivity, specificity of hub genes as a predictive biomarker for dementia prognosis. (**A**) MYC (**B**) EGFR (**C**) LNX1 (**D**) YBX1 (**E**) HSP90AA1 (**F**) ESR1 (**G**) FN1 (**H**) TK1 (**I**) ANLN (**J**) SMAD9.

polypeptide)[46], INS (insulin)[47] and MAFA (MAF bZIP transcription factor A)[48] are proved to be involved in T1DM. Altered expression of ADCYAP1 was observed to be associated with the progression of type 2 diabetes mellitus[49]. Gold et al.[50] reported that CSNK1G1 might be essential for cognitive impairment. Therefore, these genes are might be essential in the advancement of T1DM and its complications.

Furthermore, we investigated the biological functions of these DEGs by using online website, and GO and pathway enrichment analysis. Husemoen et al.[51], Zhang et al.[52], Hartz et al.[53], Słomiński et al.[54], Johansson et al.[55], Pan et al.[56], Lopez-Sanz et al.[57], Grant[58], Słomiński et al.[59], Galán et al.[60], Jordan et al.[61], Winkler et al.[62], Yip et al.[63], Crookshank et al.[64], Lempainen et al.[65], Qu and Polychronakos[66], Morrison et al.[67], Zhang et al.[68], Gerlinger-Romero et al.[69], Belanger et al.[70], Dieter et al.[71], Wanic et al.[72], Ushijima Wanic et al.[73], Guo et al.[74], Davis et al.[75], Elbarbary et al.[76], Villasenor et al.[77], Zhang et al.[78], Lee et al.[79], Zhi et al.[80], Li Calzi et al.[81], Sebastiani et al.[82], Cherney et al.[83], Doggrell[84] and Yanagihara et al.[85] studied the clinical and prognostic values of FLG (filaggrin), FGF21, PEMT (phosphatidylethanolamine *N*-methyltransferase) KL (klotho), CEL (carboxyl ester lipase), FOSL2, STAT1, TCF7L2, TP53, EGFR (epidermal growth factor receptor), ETS1, KCNJ8, DEAF1, GCG (glucagon), IKZF4, OAS1, IRS1, ABCG2, FBXO32, PTBP1, BACH2, CNDP2, KLF11, MT1E, DPP4, SLC29A3,

RGS16, MAS1, GCGR (glucagon receptor), HLA-C, VASP (vasodilator stimulated phosphoprotein), CCR2, PTGS2, GLP1R and JMJD6 in patients with T1DM. Vassilev et al.[86], Qin et al.[87], Ma et al.[88], West et al.[89], Hoffmann et al.[90], Deary et al.[91], Belangero et al.[92], Jung et al.[93], Tang et al.[94], Goodier et al.[95], Petyuk et al.[96], Roux et al.[97], Castrogiovanni et al.[98], Suleiman et al.[99], Haack et al.[100], Kwiatkowski et al.[101], Pinacho et al.[102], Luo et al.[103], He et al.[104], Moudi et al.[105], Thevenon et al.[106], Li et al.[107], Reitz et al.[108], Jenkins and Escayg[109], Letronne et al.[110], Ma et al.[111], Chabbert et al.[112], Abramsson et al.[113], Aeby et al.[114] and Roll et al.[115] showed the diagnostic values of genes include DCC (DCC netrin 1 receptor), PLP1, SNX19, SH3RF1, TNFRSF1A, NCSTN (nicastrin), DGCR2, NPAS2, CDNF (cerebral dopamine neurotrophic factor), SMCR8, HSPA2, STUB1, CHID1, ATP13A2, SQSTM1, LIG3, SP4, ACSL6, ERN1, ATF6B, LRFN2, NRG3, LRRTM3, GABRA2, ADAM30, GABRR2, TSHZ3, LOXL1, SCN1B and SRPX2 in patients with cognitive impairment. Previous studies have shown that genes include KCP (kielin cysteine rich BMP regulator)[116], NOG (noggin)[117], COL6A3[118], BTG2[119], RPS6[120], KLF15[121], KLF3[122], ZFP36[123], ETV5[124], TLE3[125], NNMT (nicotinamide N-methyltransferase)[126], WDTC1[127], ZFHX3[128], SIAH2[129], MBOAT7[130], RUNX1T1[131], MAPK4[132], KLF9[133], SELENBP1[134], HELZ2[135], ELK1[136], SERTAD2[137], CRTC3[138], ABCB11[139], TACR1[140], SLC22A11[141], PER3[142], P2RX5[143], MFAP5[144], FGL1[145], OLFM4[146], NTN1[147], ESR1[148], ABCB1[149], VAV3[150] and LAMB3[151] can be used as clinical prognostic biomarkers for obesity. Genes include STAR (steroidogenic acute regulatory protein)[152],IL1RN[153], AQP5[154], EGR1[155], SFTPD (surfactant protein D)[156], KLF10[157], PODXL (podocalyxin like)[158], FOXN3[159], IL6R[160], PBX1[161], APOD (apolipoprotein D)[162], ACVR2B[163], CD34[164], INSR (insulin receptor)[165], APOA5[166], STAR (steroidogenic acute regulatory protein)[167], PDK4[168], GLS (glutaminase)[169], FKBP5[170], SLC6A15[171], MT2A[172], SLC38A4[173], AQP7[174], ABHD15[175], ABCA1[176], ZNRF1[177], PPP1R3B[178], MAOA (monoamine oxidase A)[179], UBE2E2[180], RNASEK (ribonuclease K)[181], PREX1[182], DGKG (diacylglycerol kinase gamma)[183], POSTN (periostin)[184], COMP (cartilage oligomeric matrix protein)[185], GAP43[186], P2RY12[187], SELL (selectin L)[188] and DLG2[189] were related to type 2 diabetes mellitus. Expression of ERRFI1[190], ALOX12[191], SOCS5[192], DDIT4[193], DUSP4[194], IL6ST[195], DUSP1[196], SMAD1[197], NCL (nucleolin)[198], METTL14[199], FMOD (fibromodulin)[200], CYGB (cytoglobin)[201], UNC5A[202] and TAAR9[203] are believed to be associated with diabetic nephropathy. Genes include FAP (fibroblast activation protein alpha)[204], EYA4[205], BCL9[206], IRF2BP2[207], EGR3[208], GADD45B[209], DMD (dystrophin)[210], LSR (lipolysis stimulated lipoprotein receptor)[211], DLL4[212], SUN2[213], SOS1[214], PIK3CA[215], GAMT (guanidinoacetate *N*-methyltransferase)[216], RBM47[217], HSP90AA1[218], GAB1[219], S1PR1[220], EDNRB (endothelin receptor type B)[221], NFKBIA (NFKB inhibitor alpha)[222], GJA1[223], GADD45G[224], PHLDA1[225], CMPK2[226], FIGN (fidgetin, microtubule severing factor)[227], KCNJ2[228], ABCC9[229], DIRAS3[230], EPHX1[231], RAB4A[232], UBIAD1[233], CASQ2[234], TTN (titin)[235], KCNH1[236], JPH2[237], OXGR1[238], UCHL1[239], SERPINA3[240], MMP28[241], ADAMTS2[242], P2RY1[243], CSF2RA[244], MYO1F[245], SELPLG (selectin P ligand)[246] and SAMHD1[247] have been reported to be associated with cardiovascular disease. Previous studies had shown that the altered expression of genes include MAOB (monoamine oxidase B)[248], VEGFC (vascular endothelial growth factor C)[249], DBP (D-box binding PAR bZIP transcription factor)[250], MYADM (myeloid associated differentiation marker)[251], NES (nestin)[252], SMURF1[253], EDNRB (endothelin receptor type B)[254], MUC6[255], TOR2A[256], TNKS (tankyrase)[257], NEDD9[258], ASIC1[259], ADAMTS8[260], DYSF (dysferlin)[261], SLC26A9[262], SLC45A3[263] and KCNQ2[264] were closely related to the occurrence of hypertension. Yang et al.[265], Zhang et al.[266] and Wang et al.[267] revealed that genes include SYVN1, BTG1 and CFB (complement factor B) might be the potential targets for diabetic retinopathy diagnosis and treatment. Study indicating that these enriched genes might play important roles in the progression of T1DM.

Construction of PPI network of DEGs may be favorable for understanding the relationship of advancing T1DM. The results of the present investigation might provide potential biomarkers for the diagnosis of T1DM. SMAD9 plays an important role in the development of hypertension[268]. Our results indicate the importance of this hub gene might be involved in occurrence and development of T1DM. MYC (MYC proto-oncogene, bHLH transcription factor), LNX1, YBX1, FN1, TK1 and ANLN (anillin actin binding protein) are likely to provide new potential biomarkers for clinical practice or treatment of T1DM with further research.

In this investigation, the miRNA-hub gene regulatory network and TF-hub gene regulatory network that regulates T1DM was constructed. CDK1[269], hsa-mir-199b-3p[270], JUND[271] and FOXF2[272] are a promising biomarkers in obesity detection and diagnosis. Hsa-mir-106a-5p[273], hsa-mir-206[274], SMAD4[275] and ATF6[276] biomarkers were confirmed in type 2 diabetes mellitus progression. Hsa-mir-106a-5p[277] and HSF2[278] have been shown to promote cardiovascular disease.. Mendes-Silva et al.[279] reported that hsa-mir-664a-3p promotes cognitive impairment. Some scholars pointed out that ELF3 was involved in the pathogenesis of diabetic nephropathy[280]. Previous studies have shown that SRY is involved in the development of hypertension[281]. Our results showed that these hub genes, miRNAs and TFs are might be involved in progression of T1DM. Together, RNPS1, MAPK3, NEK6, hsa-mir-4677-3p, hsa-mir-3125, hsa-mir-4779, hsa-mir-548az-3p, hsa-mir-5688, hsa-mir-6512-3p, XAB2, KHDRBS1 and RELA might be effective targets in T1DM, but more experimental investigations and clinical trials are needed.

In conclusion, the study used a comprehensive bioinformatics analysis methods to identify DEGs, as well as unique biological functions and pathways of T1DM, thereby enhancing the current understanding of the molecular pathogenesis of T1DM. Moreover, these results might provide potential biomarkers for the initial and proper diagnosis of T1DM, as well as potential therapeutic targets for the advancementof novel T1DM treatments.

Data availability

The datasets supporting the conclusions of this article are available in the GEO (Gene Expression Omnibus) (https://www.ncbi.nlm.nih.gov/geo/) repository. [(GSE162689) (https://www.ncbi.nlm.nih.gov/geo/query/acc.cgi?acc=GSE162689].

Received: 24 September 2021; Accepted: 16 May 2022
Published online: 01 June 2022

References

1. Bekris, L. M., Kavanagh, T. J. & Lernmark, A. Targeting type 1 diabetes before and at the clinical onset of disease. *Endocr. Metab. Immune Disord. Drug Targets.* **6**(1), 103–124. https://doi.org/10.2174/187153006776056576 (2006).
2. Haller, M. J., Atkinson, M. A. & Schatz, D. Type 1 diabetes mellitus: etiology, presentation, and management. *Pediatr. Clin. N. Am.* **52**(6), 1553–1578. https://doi.org/10.1016/j.pcl.2005.07.006 (2005).
3. Maahs, D. M., West, N. A., Lawrence, J. M. & Mayer-Davis, E. J. Epidemiology of type 1 diabetes. *Endocrinol. Metab. Clin. N. Am.* **39**(3), 481–497. https://doi.org/10.1016/j.ecl.2010.05.011 (2010).
4. Akerblom, H. K., Vaarala, O., Hyöty, H., Ilonen, J. & Knip, M. Environmental factors in the etiology of type 1 diabetes. *Am. J. Med. Genet.* **115**(1), 18–29. https://doi.org/10.1002/ajmg.10340 (2002).
5. Pociot, F. & Lernmark, Å. Genetic risk factors for type 1 diabetes. *Lancet* **387**(10035), 2331–2339. https://doi.org/10.1016/S0140-6736(16)30582-7 (2016).
6. Nathan, D. M. *et al.* Intensive diabetes treatment and cardiovascular disease in patients with type 1 diabetes. *N. Engl. J. Med.* **353**(25), 2643–2653. https://doi.org/10.1056/NEJMoa052187 (2005).
7. de Boer, I. H. *et al.* Insulin therapy, hyperglycemia, and hypertension in type 1 diabetes mellitus. *Arch. Intern. Med.* **168**(17), 1867–1873. https://doi.org/10.1001/archinternmed.2008.2 (2008).
8. Hammes, H. P. *et al.* Diabetic retinopathy in type 1 diabetes-a contemporary analysis of 8,784 patients. *Diabetologia* **54**(8), 1977–1984. https://doi.org/10.1007/s00125-011-2198-1 (2011).
9. Pätäri, A. *et al.* Nephrinuria in diabetic nephropathy of type 1 diabetes. *Diabetes* **52**(12), 2969–2974. https://doi.org/10.2337/diabetes.52.12.2969 (2003).
10. González-Clemente, J. M. *et al.* Diabetic neuropathy is associated with activation of the TNF-alpha system in subjects with type 1 diabetes mellitus. *Clin. Endocrinol. (Oxf).* **63**(5), 525–529. https://doi.org/10.1111/j.1365-2265.2005.02376.x (2005).
11. Sandhu, N. *et al.* Prevalence of overweight and obesity in children and adolescents with type 1 diabetes mellitus. *J. Pediatr. Endocrinol. Metab.* **21**(7), 631–640. https://doi.org/10.1515/JPEM.2008.21.7.631 (2008).
12. Brismar, T. *et al.* Predictors of cognitive impairment in type 1 diabetes. *Psychoneuroendocrinology* **32**(8–10), 1041–1051. https://doi.org/10.1016/j.psyneuen.2007.08.002 (2007).
13. Charbonnel, B., Penfornis, A., Varroud-Vial, M., Kusnik-Joinville, O. & Detournay, B. Insulin therapy for diabetes mellitus: Treatment regimens and associated costs. *Diabetes Metab.* **38**(2), 156–163. https://doi.org/10.1016/j.diabet.2011.10.003 (2012).
14. Chang, T. J. *et al.* Vitamin D receptor gene polymorphisms influence susceptibility to type 1 diabetes mellitus in the Taiwanese population. *Clin. Endocrinol. (Oxf).* **52**(5), 575–580. https://doi.org/10.1046/j.1365-2265.2000.00985.x (2000).
15. Nejentsev, S. *et al.* Localization of type 1 diabetes susceptibility to the MHC class I genes HLA-B and HLA-A. *Nature* **450**(7171), 887–892. https://doi.org/10.1038/nature06406 (2007).
16. Thorsby, E. & Rønningen, K. S. Particular HLA-DQ molecules play a dominant role in determining susceptibility or resistance to type 1 (insulin-dependent) diabetes mellitus. *Diabetologia* **36**(5), 371–377. https://doi.org/10.1007/BF00402270 (1993).
17. Nejentsev, S. *et al.* Population-based genetic screening for the estimation of Type 1 diabetes mellitus risk in Finland: Selective genotyping of markers in the HLA-DQB1, HLA-DQA1 and HLA-DRB1 loci. *Diabet. Med.* **16**(12), 985–992. https://doi.org/10.1046/j.1464-5491.1999.00186.x (1999).
18. Barratt, B. J. *et al.* Remapping the insulin gene/IDDM2 locus in type 1 diabetes. *Diabetes* **53**(7), 1884–1889. https://doi.org/10.2337/diabetes.53.7.1884 (2004).
19. Gbr, A. A., Abdel Baky, N. A., Mohamed, E. A. & Zaky, H. S. Cardioprotective effect of pioglitazone and curcumin against diabetic cardiomyopathy in type 1 diabetes mellitus: impact on CaMKII/NF-κB/TGF-β1 and PPAR-γ signaling pathway. *Naunyn Schmiedebergs Arch. Pharmacol.* **394**(2), 349–360. https://doi.org/10.1007/s00210-020-01979-y (2021).
20. Lou, Y. *et al.* Inhibition of the Keap1/Nrf2 signaling pathway significantly promotes the progression of type 1 diabetes mellitus. *Oxid. Med. Cell Longev.* **2021**, 7866720. https://doi.org/10.1155/2021/7866720 (2021).
21. Güzel, D. *et al.* Effect of intermittent hypoxia on the cardiac HIF-1/VEGF pathway in experimental type 1 diabetes mellitus. *Anatol. J. Cardiol.* **16**(2), 76–83. https://doi.org/10.5152/akd.2015.5925 (2016).
22. Liu, H. *et al.* Downregulated NLRP3 and NLRP1 inflammasomes signaling pathways in the development and progression of type 1 diabetes mellitus. *Biomed. Pharmacother.* **94**, 619–626. https://doi.org/10.1016/j.biopha.2017.07.102 (2017).
23. Farkas, K. *et al.* Impairment of the NO/cGMP pathway in the fasting and postprandial state in type 1 diabetes mellitus. *Exp. Clin. Endocrinol. Diabetes.* **112**(5), 258–263. https://doi.org/10.1055/s-2004-817973 (2004).
24. Potter, S. S. Single-cell RNA sequencing for the study of development, physiology and disease. *Nat. Rev. Nephrol.* **14**(8), 479–492. https://doi.org/10.1038/s41581-018-0021-7 (2018).
25. Seiron, P. *et al.* Transcriptional analysis of islets of Langerhans from organ donors of different ages. *PLoS One* **16**(3), e0247888. https://doi.org/10.1371/journal.pone.0247888 (2021).
26. Clough, E. & Barrett, T. The gene expression omnibus database. *Methods Mol. Biol.* **1418**, 93–110. https://doi.org/10.1007/978-1-4939-3578-9_5 (2016).
27. Varet, H., Brillet-Guéguen, L., Coppée, J. Y. & Dillies, M. A. SARTools: A DESeq2- and EdgeR-based R pipeline for comprehensive differential analysis of RNA-Seq data. *PLoS One* **11**(6), e0157022. https://doi.org/10.1371/journal.pone.0157022 (2016).
28. Hardcastle, T. J. Generalized empirical Bayesian methods for discovery of differential data in high-throughput biology. *Bioinformatics* **32**(2), 195–202. https://doi.org/10.1093/bioinformatics/btv569 (2016).
29. Reimand, J., Kull, M., Peterson, H., Hansen, J. & Vilo, J. g:Profiler—A web-based toolset for functional profiling of gene lists from large-scale experiments. *Nucleic Acids Res.* **35**(Web Server issue), W193–W200. https://doi.org/10.1093/nar/gkm226 (2007).
30. Thomas, P. D. The gene ontology and the meaning of biological function. *Methods Mol. Biol.* **1446**, 15–24. https://doi.org/10.1007/978-1-4939-3743-1_2 (2017).
31. Fabregat, A. *et al.* The reactome pathway knowledgebase. *Nucleic Acids Res.* **46**(D1), D649–D655. https://doi.org/10.1093/nar/gkx1132 (2018).
32. Orchard, S. *et al.* The MIntAct project—IntAct as a common curation platform for 11 molecular interaction databases. *Nucleic Acids Res.* **42**, D358–D363. https://doi.org/10.1093/nar/gkt1115 (2014).
33. Shannon, P. *et al.* Ideker T Cytoscape: A software environment for integrated models of biomolecular interaction networks. *Genome Res.* **13**(11), 2498–2504. https://doi.org/10.1101/gr.1239303 (2003).
34. Przulj, N., Wigle, D. A. & Jurisica, I. Functional topology in a network of protein interactions. *Bioinformatics* **20**(3), 340–348. https://doi.org/10.1093/bioinformatics/btg415 (2004).
35. Nguyen, T. P., Liu, W. C. & Jordán, F. Inferring pleiotropy by network analysis: Linked diseases in the human PPI network. *BMC Syst. Biol.* **5**, 179. https://doi.org/10.1186/1752-0509-5-179 (2011).
36. Shi, Z. & Zhang, B. Fast network centrality analysis using GPUs. *BMC Bioinform.* **12**, 149. https://doi.org/10.1186/1471-2105-12-149 (2011).
37. Fadhal, E., Gamieldien, J. & Mwambene, E. C. Protein interaction networks as metric spaces: A novel perspective on distribution of hubs. *BMC Syst. Biol.* **8**, 6. https://doi.org/10.1186/1752-0509-8-6 (2014).

38. Zaki, N., Efimov, D. & Berengueres, J. Protein complex detection using interaction reliability assessment and weighted clustering coefficient. *BMC Bioinform.* **14**, 163. https://doi.org/10.1186/1471-2105-14 (2013).
39. Fan, Y. & Xia, J. miRNet-functional analysis and visual exploration of miRNA-target interactions in a network context. *Methods Mol. Biol.* **1819**, 215–233. https://doi.org/10.1007/978-1-4939-8618-7_10 (2018).
40. Zhou, G. *et al.* NetworkAnalyst 3.0: A visual analytics platform for comprehensive gene expression profiling and meta-analysis. *Nucleic Acids Res.* **47**, W234–W241. https://doi.org/10.1093/nar/gkz240 (2019).
41. Robin, X. *et al.* pROC: An open-source package for R and S+ to analyze and compare ROC curves. *BMC Bioinform.* **12**, 77. https://doi.org/10.1186/1471-2105-12-77 (2011).
42. Gillespie, K. M. Type 1 diabetes: Pathogenesis and prevention. *CMAJ* **175**(2), 165–170. https://doi.org/10.1503/cmaj.060244 (2006).
43. Jacquemin, B. *et al.* Common genetic polymorphisms and haplotypes of fibrinogen alpha, beta, and gamma chains affect fibrinogen levels and the response to proinflammatory stimulation in myocardial infarction survivors: The AIRGENE study. *J. Am. Coll. Cardiol.* **52**(11), 941–952. https://doi.org/10.1016/j.jacc.2008.06.016 (2008).
44. Theodoraki, E. V. *et al.* Fibrinogen beta variants confer protection against coronary artery disease in a Greek case-control study. *BMC Med. Genet.* **11**, 28. https://doi.org/10.1186/1471-2350-11-28 (2010).
45. Vafiadis, P., Bennett, S. T., Todd, J. A., Grabs, R. & Polychronakos, C. Divergence between genetic determinants of IGF2 transcription levels in leukocytes and of IDDM2-encoded susceptibility to type 1 diabetes. *J. Clin. Endocrinol. Metab.* **83**(8), 2933–2939. https://doi.org/10.1210/jcem.83.8.5048 (1998).
46. Paulsson, J. F. *et al.* High plasma levels of islet amyloid polypeptide in young with new-onset of type 1 diabetes mellitus. *PLoS One* **9**(3), e93053. https://doi.org/10.1371/journal.pone.0093053 (2014).
47. Pugliese, A. *et al.* The insulin gene is transcribed in the human thymus and transcription levels correlated with allelic variation at the INS VNTR-IDDM2 susceptibility locus for type 1 diabetes. *Nat. Genet.* **15**(3), 293–297. https://doi.org/10.1038/ng0397-293 (1997).
48. Iacovazzo, D. *et al.* MAFA missense mutation causes familial insulinomatosis and diabetes mellitus. *Proc. Natl. Acad. Sci. U. S. A.* **115**(5), 1027–1032. https://doi.org/10.1073/pnas.1712262115 (2018).
49. Gu, H. F. Genetic variation screening and association studies of the adenylate cyclase activating polypeptide 1 (ADCYAP1) gene in patients with type 2 diabetes. *Hum. Mutat.* **19**(5), 572–573. https://doi.org/10.1002/humu.9034 (2002).
50. Gold, N. B. *et al.* Heterozygous de novo variants in CSNK1G1 are associated with syndromic developmental delay and autism spectrum disorder. *Clin. Genet.* **98**(6), 571–576. https://doi.org/10.1111/cge.13851 (2020).
51. Husemoen, L. L. *et al.* No association between loss-of-function mutations in filaggrin and diabetes, cardiovascular disease, and all-cause mortality. *PLoS One* **8**(12), e84293. https://doi.org/10.1371/journal.pone.0084293 (2013).
52. Zhang, J. *et al.* The role of FGF21 in type 1 diabetes and its complications. *Int. J. Biol. Sci.* **14**(9), 1000–1011. https://doi.org/10.7150/ijbs.25026 (2018).
53. Hartz, C. S., Nieman, K. M., Jacobs, R. L., Vance, D. E. & Schalinske, K. L. Hepatic phosphatidylethanolamine *N*-methyltransferase expression is increased in diabetic rats. *J. Nutr.* **136**(12), 3005–3009. https://doi.org/10.1093/jn/136.12.3005 (2006).
54. Słomiński, B., Ryba-Stanisławowska, M., Skrzypkowska, M., Gabig-Cimińska, M. & Myśliwiec, M. A new potential mode of cardiorenal protection of KLOTHO gene variability in type 1 diabetic adolescents. *J. Mol. Med. (Berl).* **98**(7), 955–962. https://doi.org/10.1007/s00109-020-01918-7 (2020).
55. Johansson, B. B. *et al.* Diabetes and pancreatic exocrine dysfunction due to mutations in the carboxyl ester lipase gene-maturity onset diabetes of the young (CEL-MODY): A protein misfolding disease. *J. Biol. Chem.* **286**(40), 34593–34605. https://doi.org/10.1074/jbc.M111.222679 (2011).
56. Pan, S. *et al.* microRNA-143-3p contributes to inflammatory reactions by targeting FOSL2 in PBMCs from patients with autoimmune diabetes mellitus. *Acta Diabetol.* **58**(1), 63–72. https://doi.org/10.1007/s00592-020-01591-9 (2021).
57. Lopez-Sanz, L. *et al.* SOCS1-targeted therapy ameliorates renal and vascular oxidative stress in diabetes via STAT1 and PI3K inhibition. *Lab Investig.* **98**(10), 1276–1290. https://doi.org/10.1038/s41374-018-0043-6 (2018).
58. Grant, S. F. A. The TCF7L2 locus: A genetic window into the pathogenesis of type 1 and type 2 diabetes. *Diabetes Care* **42**(9), 1624–1629. https://doi.org/10.2337/dci19-0001 (2019).
59. Słomiński, B., Skrzypkowska, M., Ryba-Stanisławowska, M., Myśliwiec, M. & Trzonkowski, P. Associations of TP53 codon 72 polymorphism with complications and comorbidities in patients with type 1 diabetes. *J. Mol. Med. (Berl).* **99**(5), 675–683. https://doi.org/10.1007/s00109-020-02035-1 (2021).
60. Galán, M. *et al.* A novel role for epidermal growth factor receptor tyrosine kinase and its downstream endoplasmic reticulum stress in cardiac damage and microvascular dysfunction in type 1 diabetes mellitus. *Hypertension* **60**(1), 71–80. https://doi.org/10.1161/HYPERTENSIONAHA.112.192500 (2012).
61. Jordan, M. A., Poulton, L. D., Fletcher, J. M. & Baxter, A. G. Allelic variation of Ets1 does not contribute to NK and NKT cell deficiencies in type 1 diabetes susceptible NOD mice. *Rev. Diabet. Stud.* **6**(2), 104–116. https://doi.org/10.1900/RDS.2009.6.104 (2009).
62. Winkler, M., Lutz, R., Russ, U., Quast, U. & Bryan, J. Analysis of two KCNJ11 neonatal diabetes mutations, V59G and V59A, and the analogous KCNJ8 I60G substitution: Differences between the channel subtypes formed with SUR1. *J. Biol. Chem.* **284**(11), 6752–6762. https://doi.org/10.1074/jbc.M805435200 (2009).
63. Yip, L. *et al.* Inflammation and hyperglycemia mediate Deaf1 splicing in the pancreatic lymph nodes via distinct pathways during type 1 diabetes. *Diabetes* **64**(2), 604–617. https://doi.org/10.2337/db14-0803 (2015).
64. Crookshank, J. A. *et al.* Changes in insulin, glucagon and ER stress precede immune activation in type 1 diabetes. *J. Endocrinol.* **239**(2), 181–195. https://doi.org/10.1530/JOE-18-0328 (2018).
65. Lempainen, J. *et al.* Associations of polymorphisms in non-HLA loci with autoantibodies at the diagnosis of type 1 diabetes: INS and IKZF4 associate with insulin autoantibodies. *Pediatr Diabetes.* **14**(7), 490–496. https://doi.org/10.1111/pedi.12046 (2013).
66. Qu, H. Q., Polychronakos, C., Type I Diabetes Genetics Consortium. Reassessment of the type I diabetes association of the OAS1 locus. *Genes Immun.* **10**(Suppl 1), S69–S73. https://doi.org/10.1038/gene.2009.95 (2009).
67. Morrison, V. A., Onengut-Gumuscu, S. & Concannon, P. A functional variant of IRS1 is associated with type 1 diabetes in families from the US and UK. *Mol. Genet. Metab.* **81**(4), 291–294. https://doi.org/10.1016/j.ymgme.2003.10.018 (2004).
68. Zhang, D. *et al.* Effects of ABCG2 and SLCO1B1 gene variants on inflammation markers in patients with hypercholesterolemia and diabetes mellitus treated with rosuvastatin. *Eur. J. Clin. Pharmacol.* **76**(7), 939–946. https://doi.org/10.1007/s00228-020-02882-4 (2020).
69. Gerlinger-Romero, F., Yonamine, C. Y., Junior, D. C., Esteves, J. V. & Machado, U. F. Dysregulation between TRIM63/FBXO32 expression and soleus muscle wasting in diabetic rats: Potential role of miR-1-3p, -29a/b-3p, and -133a/b-3p. *Mol. Cell Biochem.* **427**(1–2), 187–199. https://doi.org/10.1007/s11010-016-2910-z (2017).
70. Belanger, K., Nutter, C. A., Li, J., Yu, P. & Kuyumcu-Martinez, M. N. A developmentally regulated spliced variant of PTBP1 is upregulated in type 1 diabetic hearts. *Biochem. Biophys. Res. Commun.* **509**(2), 384–389. https://doi.org/10.1016/j.bbrc.2018.12.150 (2019).
71. Dieter, C. *et al.* The rs11755527 polymorphism in the BACH2 gene and type 1 diabetes mellitus: Case control study in a Brazilian population. *Arch. Endocrinol. Metab.* **64**(2), 138–143. https://doi.org/10.20945/2359-3997000000214 (2020).

72. Wanic, K. *et al.* Exclusion of polymorphisms in carnosinase genes (CNDP1 and CNDP2) as a cause of diabetic nephropathy in type 1 diabetes: Results of large case-control and follow-up studies. *Diabetes* **57**(9), 2547–2551. https://doi.org/10.2337/db07-1303 (2008).
73. Ushijima, K. *et al.* Kawamura T;KLF11 variant in a family clinically diagnosed with early childhood-onset type 1B diabetes. *Pediatr. Diabetes.* **20**(6), 712–719. https://doi.org/10.1111/pedi.12868 (2019).
74. Guo, M. *et al.* Using hESCs to probe the interaction of the diabetes-associated genes CDKAL1 and MT1E. *Cell Rep.* **19**(8), 1512–1521. https://doi.org/10.1016/j.celrep.2017.04.070 (2017).
75. Davis, H., Jones Briscoe, V., Dumbadze, S. & Davis, S. N. Using DPP-4 inhibitors to modulate beta cell function in type 1 diabetes and in the treatment of diabetic kidney disease. *Expert. Opin. Investig. Drugs.* **28**(4), 377–388. https://doi.org/10.1080/13543784.2019.1592156 (2019).
76. Elbarbary, N. S. *et al.* An Egyptian family with H syndrome due to a novel mutation in SLC29A3 illustrating overlapping features with pigmented hypertrichotic dermatosis with insulin-dependent diabetes and Faisalabad histiocytosis. *Pediatr. Diabetes.* **14**(6), 466–472. https://doi.org/10.1111/j.1399-5448.2012.00925.x (2013).
77. Villasenor, A. *et al.* Rgs16 and Rgs8 in embryonic endocrine pancreas and mouse models of diabetes. *Dis. Model Mech.* **3**(9–10), 567–580. https://doi.org/10.1242/dmm.003210 (2010).
78. Zhang, L. *et al.* MAS-1 adjuvant immunotherapy generates robust Th2 type and regulatory immune responses providing long-term protection from diabetes in late-stage pre-diabetic NOD mice. *Autoimmunity* **47**(5), 341–350. https://doi.org/10.3109/08916934.2014.910768 (2014).
79. Lee, Y., Wang, M. Y., Du, X. Q., Charron, M. J. & Unger, R. H. Glucagon receptor knockout prevents insulin-deficient type 1 diabetes in mice. *Diabetes* **60**(2), 391–397. https://doi.org/10.2337/db10-0426 (2011).
80. Zhi, D. *et al.* Killer cell immunoglobulin-like receptor along with HLA-C ligand genes are associated with type 1 diabetes in Chinese Han population. *Diabetes Metab. Res. Rev.* **27**(8), 872–877. https://doi.org/10.1002/dmrr.1264 (2011).
81. Li Calzi, S. *et al.* Carbon monoxide and nitric oxide mediate cytoskeletal reorganization in microvascular cells via vasodilator-stimulated phosphoprotein phosphorylation: evidence for blunted responsiveness in diabetes. *Diabetes* **57**(9), 2488–2494. https://doi.org/10.2337/db08-0381 (2008).
82. Sebastiani, G. *et al.* Regulatory T-cells from pancreatic lymphnodes of patients with type-1 diabetes express increased levels of microRNA miR-125a-5p that limits CCR2 expression. *Sci. Rep.* **7**(1), 6897. https://doi.org/10.1038/s41598-017-07172-1 (2017).
83. Cherney, D. Z. *et al.* Renal hyperfiltration is a determinant of endothelial function responses to cyclooxygenase 2 inhibition in type 1 diabetes. *Diabetes Care* **33**(6), 1344–1346. https://doi.org/10.2337/dc09-2340 (2010).
84. Doggrell, S. A. Do glucagon-like peptide-1 receptor (GLP-1R) agonists have potential as adjuncts in the treatment of type 1 diabetes?. *Expert Opin. Pharmacother.* **19**(15), 1655–1661. https://doi.org/10.1080/14656566.2018.1519547 (2018).
85. Yanagihara, T., Tomino, T., Uruno, T. & Fukui, Y. Thymic epithelial cell-specific deletion of Jmjd6 reduces Aire protein expression and exacerbates disease development in a mouse model of autoimmune diabetes. *Biochem. Biophys. Res. Commun.* **489**(1), 8–13. https://doi.org/10.1016/j.bbrc.2017.05.113 (2017).
86. Vassilev, P. *et al.* Unique effects of social defeat stress in adolescent male mice on the Netrin-1/DCC pathway, prefrontal cortex dopamine and cognition (Social stress in adolescent vs. adult male mice). *Neuro* https://doi.org/10.1523/ENEURO.0045-21.2021 (2021).
87. Qin, W. *et al.* A family-based association study of PLP1 and schizophrenia. *Neurosci. Lett.* **375**(3), 207–210. https://doi.org/10.1016/j.neulet.2004.11.013 (2005).
88. Ma, L. *et al.* Schizophrenia risk variants influence multiple classes of transcripts of sorting nexin 19 (SNX19). *Mol. Psychiatry.* **25**(4), 831–843. https://doi.org/10.1038/s41380-018-0293-0 (2020).
89. West, R. J. H., Ugbode, C., Gao, F. B. & Sweeney, S. T. The pro-apoptotic JNK scaffold POSH/SH3RF1 mediates CHMP2BIntron5-associated toxicity in animal models of frontotemporal dementia. *Hum. Mol. Genet.* **27**(8), 1382–1395. https://doi.org/10.1093/hmg/ddy048 (2018).
90. Hoffmann, L. A. *et al.* TNFRSF1A R92Q mutation in association with a multiple sclerosis-like demyelinating syndrome. *Neurology* **70**(13 Pt 2), 1155–1156. https://doi.org/10.1212/01.wnl.0000296279.98236.8a (2008).
91. Deary, I. J. *et al.* Nicastrin gene polymorphisms, cognitive ability level and cognitive ageing. *Neurosci. Lett.* **373**(2), 110–114. https://doi.org/10.1016/j.neulet.2004.09.073 (2005).
92. Belangero, S. I. *et al.* DGCR2 influences cortical thickness through a mechanism independent of schizophrenia pathogenesis. *Psychiatry Res.* **274**, 391–394. https://doi.org/10.1016/j.psychres.2019.02.068 (2019).
93. Jung, J. S. *et al.* Association between restless legs syndrome and CLOCK and NPAS2 gene polymorphisms in schizophrenia. *Chronobiol. Int.* **31**(7), 838–844. https://doi.org/10.3109/07420528.2014.914034 (2014).
94. Tang, T., Li, Y., Jiao, Q., Du, X. & Jiang, H. Cerebral dopamine neurotrophic factor: A potential therapeutic agent for Parkinson's disease. *Neurosci. Bull.* **33**(5), 568–575. https://doi.org/10.1007/s12264-017-0123-4 (2017).
95. Goodier, J. L. *et al.* C9orf72-associated SMCR8 protein binds in the ubiquitin pathway and with proteins linked with neurological disease. *Acta Neuropathol. Commun.* **8**(1), 110. https://doi.org/10.1186/s40478-020-00982-x (2020).
96. Petyuk, V. A. *et al.* The human brainome: network analysis identifies HSPA2 as a novel Alzheimer's disease target. *Brain* **141**(9), 2721–2739. https://doi.org/10.1093/brain/awy215 (2018).
97. Roux, T. *et al.* Clinical, neuropathological, and genetic characterization of STUB1 variants in cerebellar ataxias: A frequent cause of predominant cognitive impairment. *Genet. Med.* **22**(11), 1851–1862. https://doi.org/10.1038/s41436-020-0899-x (2020).
98. Castrogiovanni, P. *et al.* Brain CHID1 expression correlates with NRGN and CALB1 in healthy subjects and AD patients. *Cells* **10**(4), 882. https://doi.org/10.3390/cells10040882 (2021).
99. Suleiman, J., Hamwi, N. & El-Hattab, A. W. ATP13A2 novel mutations causing a rare form of juvenile-onset Parkinson disease. *Brain Dev.* **40**(9), 824–826. https://doi.org/10.1016/j.braindev.2018.05.017 (2018).
100. Haack, T. B. *et al.* Absence of the autophagy adaptor SQSTM1/p62 causes childhood-onset neurodegeneration with ataxia, dystonia, and gaze palsy. *Am. J. Hum. Genet.* **99**(3), 735–743. https://doi.org/10.1016/j.ajhg.2016.06.026 (2016).
101. Kwiatkowski, D. *et al.* Association between single-nucleotide polymorphisms of the hOGG1, NEIL1, APEX1, FEN1, LIG1, and LIG3 genes and Alzheimer's disease risk. *Neuropsychobiology* **73**(2), 98–107. https://doi.org/10.1159/000444643 (2016).
102. Pinacho, R. *et al.* Increased SP4 and SP1 transcription factor expression in the postmortem hippocampus of chronic schizophrenia. *J. Psychiatr. Res.* **58**, 189–196. https://doi.org/10.1016/j.jpsychires.2014.08.006 (2014).
103. Luo, X. J. *et al.* Association of haplotypes spanning PDZ-GEF2, LOC728637 and ACSL6 with schizophrenia in Han Chinese. *J. Med. Genet.* **45**(12), 818–826. https://doi.org/10.1136/jmg.2008.060657 (2008).
104. He, L. *et al.* Exome-wide age-of-onset analysis reveals exonic variants in ERN1 and SPPL2C associated with Alzheimer's disease. *Transl. Psychiatry.* **11**(1), 146. https://doi.org/10.1038/s41398-021-01263-4 (2021).
105. Moudi, M. *et al.* Polymorphism in the 3'-UTR of LIF but Not in the ATF6B gene associates with schizophrenia susceptibility: A case-control study and in silico analyses. *J. Mol. Neurosci.* **70**(12), 2093–2101. https://doi.org/10.1007/s12031-020-01616-6 (2020).
106. Thevenon, J. *et al.* Heterozygous deletion of the LRFN2 gene is associated with working memory deficits. *Eur. J. Hum. Genet.* **24**(6), 911–918. https://doi.org/10.1038/ejhg.2015.221 (2016).
107. Li, Z. *et al.* NRG3 contributes to cognitive deficits in chronic patients with schizophrenia. *Schizophr. Res.* **215**, 134–139. https://doi.org/10.1016/j.schres.2019.10.060 (2020).

108. Reitz, C., Conrad, C., Roszkowski, K., Rogers, R. S. & Mayeux, R. Effect of genetic variation in LRRTM3 on risk of Alzheimer disease. *Arch. Neurol.* **69**(7), 894–900. https://doi.org/10.1001/archneurol.2011.2463 (2012).
109. Jenkins, A. & Escayg, A. Reply: Novel GABRA2 variants in epileptic encephalopathy and intellectual disability with seizures. *Brain* **142**(5), e16. https://doi.org/10.1093/brain/awz086 (2019).
110. Letronne, F. *et al.* ADAM30 downregulates APP-linked defects through cathepsin D activation in Alzheimer's disease. *EBioMedicine* **9**, 278–292. https://doi.org/10.1016/j.ebiom.2016.06.002 (2016).
111. Ma, Z. *et al.* Genetic polymorphism of GABRR2 modulates individuals' general cognitive ability in healthy Chinese Han People. *Cell Mol. Neurobiol.* **37**(1), 93–100. https://doi.org/10.1007/s10571-016-0347-2 (2017).
112. Chabbert, D. *et al.* Postnatal Tshz3 deletion drives altered corticostriatal function and autism spectrum disorder-like behavior. *Biol. Psychiatry.* **86**(4), 274–285. https://doi.org/10.1016/j.biopsych.2019.03.974 (2019).
113. Abramsson, A. *et al.* No association of LOXL1 gene polymorphisms with Alzheimer's disease. *Neuromol. Med.* **13**(2), 160–166. https://doi.org/10.1007/s12017-011-8144-z (2011).
114. Aeby, A. *et al.* SCN1B-linked early infantile developmental and epileptic encephalopathy. *Ann. Clin. Transl. Neurol.* **6**(12), 2354–2367. https://doi.org/10.1002/acn3.50921 (2019).
115. Roll, P. *et al.* SRPX2 mutations in disorders of language cortex and cognition. *Hum. Mol. Genet.* **15**(7), 1195–1207. https://doi.org/10.1093/hmg/ddl035 (2006).
116. Soofi, A. *et al.* The kielin/chordin-like protein (KCP) attenuates high-fat diet-induced obesity and metabolic syndrome in mice. *J. Biol. Chem.* **292**(22), 9051–9062. https://doi.org/10.1074/jbc.M116.771428 (2017).
117. Blázquez-Medela, A. M. *et al.* Noggin depletion in adipocytes promotes obesity in mice. *Mol. Metab.* **25**, 50–63. https://doi.org/10.1016/j.molmet.2019.04.004 (2019).
118. McCulloch, L. J. *et al.* COL6A3 is regulated by leptin in human adipose tissue and reduced in obesity. *Endocrinology* **156**(1), 134–146. https://doi.org/10.1210/en.2014-1042 (2015).
119. Gan, M. *et al.* Genistein inhibits high fat diet-induced obesity through miR-222 by targeting BTG2 and adipor1. *Food Funct.* **11**(3), 2418–2426. https://doi.org/10.1039/c9fo00861f (2020).
120. Han, X., Guo, J., You, Y., Zhan, J. & Huang, W. p-Coumaric acid prevents obesity via activating thermogenesis in brown adipose tissue mediated by mTORC1-RPS6. *FASEB J.* **34**(6), 7810–7824. https://doi.org/10.1096/fj.202000333R (2020).
121. Wang, G. *et al.* Teneligliptin promotes bile acid synthesis and attenuates lipid accumulation in obese mice by targeting the KLF15-Fgf15 pathway. *Chem. Res. Toxicol.* **33**(8), 2164–2171. https://doi.org/10.1021/acs.chemrestox.0c00192 (2020).
122. Zhou, X. *et al.* miR-324-5p promotes adipocyte differentiation and lipid droplet accumulation by targeting Krueppel-like factor 3 (KLF3). *J. Cell Physiol.* **235**(10), 7484–7495. https://doi.org/10.1002/jcp.29652 (2020).
123. Caracciolo, V. *et al.* Myeloid-specific deletion of Zfp36 protects against insulin resistance and fatty liver in diet-induced obese mice. *Am. J. Physiol. Endocrinol. Metab.* **315**(4), E676–E693. https://doi.org/10.1152/ajpendo.00224.2017 (2018).
124. Lv, D., Zhou, D., Zhang, Y., Zhang, S. & Zhu, Y. M. Two obesity susceptibility loci in LYPLAL1 and ETV5 independently associated with childhood hypertension in Chinese population. *Gene* **627**, 284–289. https://doi.org/10.1016/j.gene.2017.06.030 (2017).
125. Pearson, S. *et al.* Loss of TLE3 promotes the mitochondrial program in beige adipocytes and improves glucose metabolism. *Genes Dev.* **33**(13–14), 747–762. https://doi.org/10.1101/gad.321059.118 (2019).
126. Brachs, S. *et al.* Genetic nicotinamide *N*-methyltransferase (Nnmt) deficiency in male mice improves insulin sensitivity in diet-induced obesity but does not affect glucose tolerance. *Diabetes* **68**(3), 527–542. https://doi.org/10.2337/db18-0780 (2019).
127. Lai, C. Q. *et al.* WDTC1, the ortholog of Drosophila adipose gene, associates with human obesity, modulated by MUFA intake. *Obesity (Silver Spring)* **17**(3), 593–600. https://doi.org/10.1038/oby.2008.561 (2009).
128. Yang, S. A. Association study between ZFHX3 gene polymorphisms and obesity in Korean population. *J. Exerc Rehabil.* **13**(4), 491–494. https://doi.org/10.12965/jer.1735080.540 (2017).
129. Kilroy, G. *et al.* The ubiquitin ligase Siah2 regulates obesity-induced adipose tissue inflammation. *Obesity (Silver Spring)* **23**(11), 2223–2232. https://doi.org/10.1002/oby.21220 (2015).
130. Zusi, C. *et al.* Association between MBOAT7 rs641738 polymorphism and non-alcoholic fatty liver in overweight or obese children. *Nutr. Metab. Cardiovasc. Dis.* **31**(5), 1548–1555. https://doi.org/10.1016/j.numecd.2021.01.020 (2021).
131. Zhou, Y., Hambly, B. D., Simmons, D. & McLachlan, C. S. RUNX1T1 rs34269950 is associated with obesity and metabolic syndrome. *QJM* https://doi.org/10.1093/qjmed/hcaa208 (2020).
132. Gao, Y. *et al.* MiR-127 attenuates adipogenesis by targeting MAPK4 and HOXC6 in porcine adipocytes. *J. Cell Physiol.* **234**(12), 21838–21850. https://doi.org/10.1002/jcp.28660 (2019).
133. Wei, Z. *et al.* MiR-142-3p inhibits adipogenic differentiation and autophagy in obesity through targeting KLF9. *Mol. Cell Endocrinol.* **518**, 111028. https://doi.org/10.1016/j.mce.2020.111028 (2020).
134. Randi, E. B., Casili, G., Jacquemai, S. & Szabo, C. Selenium-binding protein 1 (SELENBP1) supports hydrogen sulfide biosynthesis and adipogenesis. *Antioxidants (Basel).* **10**(3), 361. https://doi.org/10.3390/antiox10030361 (2021).
135. Yoshino, S. *et al.* Protection against high-fat diet-induced obesity in Helz2-deficient male mice due to enhanced expression of hepatic leptin receptor. *Endocrinology* **155**(9), 3459–3472. https://doi.org/10.1210/en.2013-2160 (2014).
136. Pang, L. *et al.* miR-1275 inhibits adipogenesis via ELK1 and its expression decreases in obese subjects. *J. Mol. Endocrinol.* **57**(1), 33–43. https://doi.org/10.1530/JME-16-0007 (2016).
137. Chen, C. *et al.* miR-128-3p regulates 3T3-L1 adipogenesis and lipolysis by targeting Pparg and Sertad2. *J. Physiol. Biochem.* **74**(3), 381–393. https://doi.org/10.1007/s13105-018-0625-1 (2018).
138. Prats-Puig, A. *et al.* Soluble CRTC3: A newly identified protein released by adipose tissue that is associated with childhood obesity. *Clin. Chem.* **62**(3), 476–484. https://doi.org/10.1373/clinchem.2015.249136 (2016).
139. Henkel, A. S. *et al.* Hepatic overexpression of abcb11 promotes hypercholesterolemia and obesity in mice. *Gastroenterology* **141**(4), 1404-1411.e14112. https://doi.org/10.1053/j.gastro.2011.06.062 (2011).
140. Klöting, N., Wilke, B. & Klöting, I. Alleles on rat chromosome 4 (D4Got41-Fabp1/Tacr1) regulate subphenotypes of obesity. *Obes. Res.* **13**(3), 589–595. https://doi.org/10.1038/oby.2005.63 (2005).
141. Giri, A. K. *et al.* Multifaceted genome-wide study identifies novel regulatory loci in SLC22A11 and ZNF45 for body mass index in Indians. *Mol. Genet. Genom.* **295**(4), 1013–1026. https://doi.org/10.1007/s00438-020-01678-6 (2020).
142. Samblas, M. *et al.* PTPRS and PER3 methylation levels are associated with childhood obesity: Results from a genome-wide methylation analysis. *Pediatr. Obes.* **13**(3), 149–158. https://doi.org/10.1111/ijpo.12224 (2018).
143. Ussar, S. *et al.* ASC-1, PAT2, and P2RX5 are cell surface markers for white, beige, and brown adipocytes. *Sci. Transl. Med.* **6**(247), 247ra103. https://doi.org/10.1126/scitranslmed.3008490 (2014).
144. Vaittinen, M. *et al.* MFAP5 is related to obesity-associated adipose tissue and extracellular matrix remodeling and inflammation. *Obesity (Silver Spring)* **23**(7), 1371–1378. https://doi.org/10.1002/oby.21103 (2015).
145. Wu, H. T. *et al.* Targeting fibrinogen-like protein 1 is a novel therapeutic strategy to combat obesity. *FASEB J.* **34**(2), 2958–2967. https://doi.org/10.1096/fj.201901925R (2020).
146. Albuquerque, D., Nóbrega, C., Rodríguez-López, R. & Manco, L. Association study of common polymorphisms in MSRA, TFAP2B, MC4R, NRXN3, PPARGC1A, TMEM18, SEC16B, HOXB5 and OLFM4 genes with obesity-related traits among Portuguese children. *J. Hum. Genet.* **59**(6), 307–313. https://doi.org/10.1038/jhg.2014.23 (2014).
147. Sharma, M. *et al.* Netrin-1 alters adipose tissue macrophage fate and function in obesity. *Immunometabolism.* **1**(2), e190010. https://doi.org/10.20900/immunometab20190010 (2019).

148. Guclu-Geyik, F., Coban, N., Can, G. & Erginel-Unaltuna, N. The rs2175898 polymorphism in the ESR1 gene has a significant sex-specific effect on obesity. *Biochem. Genet.* **58**(6), 935–952. https://doi.org/10.1007/s10528-020-09987-6 (2020).
149. Ichihara, S. *et al.* Association of a polymorphism of ABCB1 with obesity in Japanese individuals. *Genomics* **91**(6), 512–516. https://doi.org/10.1016/j.ygeno.2008.03.004 (2008).
150. Menacho-Márquez, M. *et al.* Chronic sympathoexcitation through loss of Vav3, a Rac1 activator, results in divergent effects on metabolic syndrome and obesity depending on diet. *Cell Metab.* **18**(2), 199–211. https://doi.org/10.1016/j.cmet.2013.07.001 (2013).
151. Jiao, H. *et al.* Whole-exome sequencing suggests LAMB3 as a susceptibility gene for morbid obesity. *Diabetes* **65**(10), 2980–2989. https://doi.org/10.2337/db16-052 (2016).
152. Qiu, Y. *et al.* Steroidogenic acute regulatory protein (StAR) overexpression attenuates HFD-induced hepatic steatosis and insulin resistance. *Biochim. Biophys. Acta Mol. Basis Dis.* **1863**(4), 978–990. https://doi.org/10.1016/j.bbadis.2017.01.026 (2017).
153. Margaryan, S., Kriegova, E., Fillerova, R., Smotkova Kraiczova, V. & Manukyan, G. Hypomethylation of IL1RN and NFKB1 genes is linked to the dysbalance in IL1β/IL-1Ra axis in female patients with type 2 diabetes mellitus. *PLoS One* **15**(5), e0233737. https://doi.org/10.1371/journal.pone.0233737 (2020).
154. Gao, C. & Zhang, W. Urinary AQP5 is independently associated with eGFR decline in patients with type 2 diabetes and nephropathy. *Diabetes Res. Clin. Pract.* **155**, 107805. https://doi.org/10.1016/j.diabres.2019.107805 (2019).
155. Wu, J. *et al.* Egr-1 transcriptionally activates protein phosphatase PTP1B to facilitate hyperinsulinemia-induced insulin resistance in the liver in type 2 diabetes. *FEBS Lett.* **593**(21), 3054–3063. https://doi.org/10.1002/1873-3468.13537 (2019).
156. Pueyo, N. *et al.* Common genetic variants of surfactant protein-D (SP-D) are associated with type 2 diabetes. *PLoS One* **8**(4), e60468. https://doi.org/10.1371/journal.pone.0060468 (2013).
157. Gutierrez-Aguilar, R. *et al.* Minor contribution of SMAD7 and KLF10 variants to genetic susceptibility of type 2 diabetes. *Diabetes Metab.* **33**(5), 372–378. https://doi.org/10.1016/j.diabet.2007.06.002 (2007).
158. El-Ashmawy, H. M., Selim, F. O., Hosny, T. A. M. & Almassry, H. N. Association of serum podocalyxin levels with peripheral arterial disease in patients with type 2 diabetes. *J. Diabetes Complicat.* **33**(7), 495–499. https://doi.org/10.1016/j.jdiacomp.2019.04.003 (2019).
159. Erickson, M. L., Karanth, S., Ravussin, E. & Schlegel, A. FOXN3 hyperglycemic risk allele and insulin sensitivity in humans. *BMJ Open Diabetes Res. Care.* **7**(1), e000688. https://doi.org/10.1136/bmjdrc-2019-000688 (2019).
160. Wu, X. *et al.* IL6R inhibits viability and apoptosis of pancreatic beta-cells in type 2 diabetes mellitus via regulation by miR-22 of the JAK/STAT signaling pathway. *Diabetes Metab. Syndr. Obes.* **12**, 1645–1657. https://doi.org/10.2147/DMSO.S211700 (2019).
161. Duesing, K. *et al.* Evaluating the association of common PBX1 variants with type 2 diabetes. *BMC Med. Genet.* **9**, 14. https://doi.org/10.1186/1471-2350-9-14 (2008).
162. Do Carmo, S., Fournier, D., Mounier, C. & Rassart, E. Human apolipoprotein D overexpression in transgenic mice induces insulin resistance and alters lipid metabolism. *Am. J. Physiol. Endocrinol. Metab.* **296**(4), E802–E811. https://doi.org/10.1152/ajpendo.90725.2008 (2009).
163. Dupont, S. *et al.* No evidence for linkage or for diabetes-associated mutations in the activin type 2B receptor gene (ACVR2B) in French patients with mature-onset diabetes of the young or type 2 diabetes. *Diabetes* **50**(5), 1219–1221. https://doi.org/10.2337/diabetes.50.5.1219 (2001).
164. Tripaldi, R. *et al.* Endogenous PCSK9 may influence circulating CD45neg/CD34bright and CD45neg/CD34bright/CD146neg cells in patients with type 2 diabetes mellitus. *Sci. Rep.* **11**(1), 9659. https://doi.org/10.1038/s41598-021-88941-x (2021).
165. Parvin, M. *et al.* Functional polymorphism located in the microRNA binding site of the insulin receptor (INSR) gene confers risk for type 2 diabetes mellitus in the Bangladeshi population. *Biochem. Genet.* **57**(1), 20–33. https://doi.org/10.1007/s10528-018-9872-7 (2019).
166. Weber, K. S. *et al.* Associations between explorative dietary patterns and serum lipid levels and their interactions with ApoA5 and ApoE haplotype in patients with recently diagnosed type 2 diabetes. *Cardiovasc. Diabetol.* **15**(1), 138. https://doi.org/10.1186/s12933-016-0455-9 (2016).
167. Qiu, Y. *et al.* Steroidogenic acute regulatory protein (StAR) overexpression reduces inflammation and insulin resistance in obese mice. *J. Cell Biochem.* **118**(11), 3932–3942. https://doi.org/10.1002/jcb.26046 (2017).
168. Mori, J. *et al.* ANG II causes insulin resistance and induces cardiac metabolic switch and inefficiency: A critical role of PDK4. *Am. J. Physiol. Heart Circ. Physiol.* **304**(8), H1103–H1113. https://doi.org/10.1152/ajpheart.00636.2012 (2013).
169. Griffin, J. W. D., Liu, Y., Bradshaw, P. C. & Wang, K. In silico preliminary association of ammonia metabolism genes GLS, CPS1, and GLUL with risk of Alzheimer's disease, major depressive disorder, and type 2 diabetes. *J. Mol. Neurosci.* **64**(3), 385–396. https://doi.org/10.1007/s12031-018-1035-0 (2018).
170. Sidibeh, C. O. *et al.* FKBP5 expression in human adipose tissue: potential role in glucose and lipid metabolism, adipogenesis and type 2 diabetes. *Endocrine* **62**(1), 116–128. https://doi.org/10.1007/s12020-018-1674-5 (2018).
171. Haydar, S. *et al.* Fine-scale haplotype mapping of MUT, AACS, SLC6A15 and PRKCA genes indicates association with insulin resistance of metabolic syndrome and relationship with branched chain amino acid metabolism or regulation. *PLoS One* **14**(3), e0214122. https://doi.org/10.1371/journal.pone.0214122 (2019).
172. Yang, L. *et al.* Polymorphisms in metallothionein-1 and -2 genes associated with the risk of type 2 diabetes mellitus and its complications. *Am. J. Physiol. Endocrinol. Metab.* **294**(5), E987–E992. https://doi.org/10.1152/ajpendo.90234.2008 (2008).
173. González-Renteria, S. M. *et al.* Association of the polymorphisms 292 C>T and 1304 G>A in the SLC38A4 gene with hyperglycaemia. *Diabetes Metab. Res. Rev.* **29**(1), 39–43. https://doi.org/10.1002/dmrr.2344 (2013).
174. Lebeck, J., Søndergaard, E. & Nielsen, S. Increased AQP7 abundance in skeletal muscle from obese men with type 2 diabetes. *Am. J. Physiol. Endocrinol. Metab.* **315**(3), E367–E373. https://doi.org/10.1152/ajpendo.00468.2017 (2018).
175. Xia, W. *et al.* Loss of ABHD15 impairs the anti-lipolytic action of insulin by altering PDE3B stability and contributes to insulin resistance. *Cell Rep.* **23**(7), 1948–1961. https://doi.org/10.1016/j.celrep.2018.04.055 (2018).
176. Ben Aissa, M. *et al.* Discovery of nonlipogenic ABCA1 inducing compounds with potential in Alzheimer's disease and type 2 diabetes. *ACS Pharmacol. Transl. Sci.* **4**(1), 143–154. https://doi.org/10.1021/acsptsci.0c00149 (2021).
177. Peng, D. *et al.* Common variants in or near ZNRF1, COLEC12, SCYL1BP1 and API5 are associated with diabetic retinopathy in Chinese patients with type 2 diabetes. *Diabetologia* **58**(6), 1231–1238. https://doi.org/10.1007/s00125-015-3569-9 (2015).
178. Manning, A. K. *et al.* A long non-coding RNA, LOC157273, is an effector transcript at the chromosome 8p23.1-PPP1R3B metabolic traits and type 2 diabetes risk locus. *Front. Genet.* **11**, 615. https://doi.org/10.3389/fgene.2020.00615 (2020).
179. Ganic, E., Johansson, J. K., Bennet, H., Fex, M. & Artner, I. Islet-specific monoamine oxidase A and B expression depends on MafA transcriptional activity and is compromised in type 2 diabetes. *Biochem. Biophys. Res. Commun.* **468**(4), 629–635. https://doi.org/10.1016/j.bbrc.2015.11.002 (2015).
180. Plengvidhya, N. *et al.* Impact of KCNQ1, CDKN2A/2B, CDKAL1, HHEX, MTNR1B, SLC30A8, TCF7L2, and UBE2E2 on risk of developing type 2 diabetes in Thai population. *BMC Med. Genet.* **19**(1), 93. https://doi.org/10.1186/s12881-018-0614-9 (2018).
181. Traurig, M. *et al.* Analysis of SLC16A11 variants in 12,811 American Indians: Genotype-obesity interaction for type 2 diabetes and an association with RNASEK expression. *Diabetes* **65**(2), 510–519. https://doi.org/10.2337/db15-0571 (2016).
182. Lewis, J. P. *et al.* Analysis of candidate genes on chromosome 20q12-13.1 reveals evidence for BMI mediated association of PREX1 with type 2 diabetes in European Americans. *Genomics* **96**(4), 211–219. https://doi.org/10.1016/j.ygeno.2010.07.006 (2010).

183. Mannerås-Holm, L., Kirchner, H., Björnholm, M., Chibalin, A. V. & Zierath, J. R. mRNA expression of diacylglycerol kinase isoforms in insulin-sensitive tissues: Effects of obesity and insulin resistance. *Physiol. Rep.* **3**(4), e12372. https://doi.org/10.14814/phy2.12372 (2015).
184. Luo, Y. *et al.* Plasma periostin levels are increased in chinese subjects with obesity and type 2 diabetes and are positively correlated with glucose and lipid parameters. *Mediat. Inflamm.* **2016**, 6423637. https://doi.org/10.1155/2016/6423637 (2016).
185. Arellano Perez Vertti, R. D., Aguilar Muñiz, L. S., Morán Martínez, J., González Galarza, F. F. & Arguello, A. R. Cartilage oligomeric matrix protein levels in type 2 diabetes associated with primary knee osteoarthritis patients. *Genet. Test Mol. Biomark.* **23**(1), 16–22. https://doi.org/10.1089/gtmb.2018.0184 (2019).
186. Bursova, S. *et al.* Expression of growth-associated protein 43 in the skin nerve fibers of patients with type 2 diabetes mellitus. *J. Neurol. Sci.* **315**(1–2), 60–63. https://doi.org/10.1016/j.jns.2011.11.038 (2012).
187. Fejes, Z. *et al.* Hyperglycaemia suppresses microRNA expression in platelets to increase P2RY12 and SELP levels in type 2 diabetes mellitus. *Thromb. Haemost.* **117**(3), 529–542. https://doi.org/10.1160/TH16-04-0322 (2017).
188. Stavarachi, M. *et al.* Investigation of P213S SELL gene polymorphism in type 2 diabetes mellitus and related end stage renal disease. A case-control study. *Rom. J. Morphol. Embryol.* **52**(3 Suppl), 995–998 (2011).
189. Yang, C. H. *et al.* E2f8 and Dlg2 genes have independent effects on impaired insulin secretion associated with hyperglycaemia. *Diabetologia* **63**(7), 1333–1348. https://doi.org/10.1007/s00125-020-05137-0 (2020).
190. Lee, I. S. *et al.* Novel ERBB receptor feedback inhibitor 1 (ERRFI1) + 808 T/G polymorphism confers protective effect on diabetic nephropathy in a Korean population. *Dis. Mark.* **34**(2), 113–124. https://doi.org/10.3233/DMA-120949 (2013).
191. Roumeliotis, A. K. *et al.* Association of ALOX12 gene polymorphism with all-cause and cardiovascular mortality in diabetic nephropathy. *Int. Urol. Nephrol.* **50**(2), 321–329. https://doi.org/10.1007/s11255-017-1755-z (2018).
192. Tsai, Y. C. *et al.* Angpt2 induces mesangial cell apoptosis through the microRNA-33-5p-SOCS5 loop in diabetic nephropathy. *Mol. Ther. Nucleic Acids.* **13**, 543–555. https://doi.org/10.1016/j.omtn.2018.10.003 (2018).
193. Wang, H. *et al.* In vitro and in vivo inhibition of mTOR by 1,25-dihydroxyvitamin D3 to improve early diabetic nephropathy via the DDIT4/TSC2/mTOR pathway. *Endocrine* **54**(2), 348–359. https://doi.org/10.1007/s12020-016-0999-1 (2016).
194. Denhez, B. *et al.* Diabetes-induced DUSP4 reduction promotes podocyte dysfunction and progression of diabetic nephropathy. *Diabetes* **68**(5), 1026–1039. https://doi.org/10.2337/db18-0837 (2019).
195. Huang, H., Zhang, G. & Ge, Z. lncRNA MALAT1 promotes renal fibrosis in diabetic nephropathy by targeting the miR-2355-3p/IL6ST axis. *Front. Pharmacol.* **12**, 647650. https://doi.org/10.3389/fphar.2021.647650 (2021).
196. Sheng, J. *et al.* DUSP1 recuses diabetic nephropathy via repressing JNK-Mff-mitochondrial fission pathways. *J. Cell Physiol.* **234**(3), 3043–3057. https://doi.org/10.1002/jcp.27124 (2019).
197. Doi, T. *et al.* Urinary IgG4 and Smad1 are specific biomarkers for renal structural and functional changes in early stages of diabetic nephropathy. *Diabetes* **67**(5), 986–993. https://doi.org/10.2337/db17-1043 (2018).
198. Wang, S. *et al.* Long non-coding RNA CYP4B1-PS1-001 inhibits proliferation and fibrosis in diabetic nephropathy by interacting with nucleolin. *Cell Physiol. Biochem.* **49**(6), 2174–2187. https://doi.org/10.1159/000493821 (2018).
199. Xu, Z. *et al.* METTL14-regulated PI3K/Akt signaling pathway via PTEN affects HDAC5-mediated epithelial-mesenchymal transition of renal tubular cells in diabetic kidney disease. *Cell Death Dis.* **12**(1), 32. https://doi.org/10.1038/s41419-020-03312-0 (2021).
200. Feng, S. *et al.* Identification of lumican and fibromodulin as hub genes associated with accumulation of extracellular matrix in diabetic nephropathy. *Kidney Blood Press. Res.* https://doi.org/10.1159/000514013 (2021).
201. Xu, Z. J. *et al.* Liuwei Dihuang pill treats diabetic nephropathy in rats by inhibiting of TGF-β/SMADS, MAPK, and NF-kB and upregulating expression of cytoglobin in renal tissues. *Medicine (Baltimore)* **96**(3), e5879. https://doi.org/10.1097/MD.0000000000005879 (2017).
202. Jiao, X. *et al.* Netrin-1 works with UNC5B to regulate angiogenesis in diabetic kidney disease. *Front. Med.* **14**(3), 293–304. https://doi.org/10.1007/s11684-019-0715-7 (2020).
203. Ruiz-Hernández, A. *et al.* Diabetic nephropathy produces alterations in the tissue expression profile of the orphan receptors GPR149, GPR153, GPR176, TAAR3, TAAR5 and TAAR9 in Wistar rats. *Nucleosides Nucleotides Nucleic Acids.* **39**(8), 1150–1161. https://doi.org/10.1080/15257770.2020.1780437 (2020).
204. Heckmann, M. B. *et al.* Relationship between cardiac fibroblast activation protein activity by positron emission tomography and cardiovascular disease. *Circ. Cardiovasc. Imaging.* **13**(9), e010628. https://doi.org/10.1161/CIRCIMAGING.120.010628 (2020).
205. Williams, T. *et al.* Eya4 induces hypertrophy via regulation of p27kip1. *Circ. Cardiovasc. Genet.* **8**(6), 752–764. https://doi.org/10.1161/CIRCGENETICS.115.001134 (2015).
206. Cantù, C. *et al.* Mutations in Bcl9 and Pygo genes cause congenital heart defects by tissue-specific perturbation of Wnt/β-catenin signaling. *Genes Dev.* **32**(21–22), 1443–1458. https://doi.org/10.1101/gad.315531.118 (2018).
207. Chen, H. H. *et al.* IRF2BP2 reduces macrophage inflammation and susceptibility to atherosclerosis. *Circ. Res.* **117**(8), 671–683. https://doi.org/10.1161/CIRCRESAHA.114.305777 (2015).
208. Li, X. *et al.* Association of Egr3 genetic polymorphisms and coronary artery disease in the Uygur and Han of China. *Lipids Health Dis.* **13**, 84. https://doi.org/10.1186/1476-511X-13-84 (2014).
209. Wang, J. *et al.* GADD45B inhibits MKK7-induced cardiac hypertrophy and the polymorphisms of GADD45B is associated with inter-ventricular septum hypertrophy. *Biochem. Biophys. Res. Commun.* **372**(4), 623–628. https://doi.org/10.1016/j.bbrc.2008.05.122 (2008).
210. Rodriguez-Gonzalez, M., Lubian-Gutierrez, M., Cascales-Poyatos, H. M., Perez-Reviriego, A. A. & Castellano-Martinez, A. Role of the renin–angiotensin-aldosterone system in dystrophin-deficient cardiomyopathy. *Int. J. Mol. Sci.* **22**(1), 356. https://doi.org/10.3390/ijms22010356 (2020).
211. Yen, F. T. *et al.* Lipolysis stimulated lipoprotein receptor: A novel molecular link between hyperlipidemia, weight gain, and atherosclerosis in mice. *J. Biol. Chem.* **283**(37), 25650–25659. https://doi.org/10.1074/jbc.M801027200 (2008).
212. Nakano, T. *et al.* Uremic Toxin indoxyl sulfate promotes proinflammatory macrophage activation via the interplay of OATP2B1 and Dll4-notch signaling. *Circulation* **139**(1), 78–96. https://doi.org/10.1161/CIRCULATIONAHA.118.034588 (2019).
213. Stewart, R. M., Rodriguez, E. C. & King, M. C. Ablation of SUN2-containing LINC complexes drives cardiac hypertrophy without interstitial fibrosis. *Mol. Biol. Cell.* **30**(14), 1664–1675. https://doi.org/10.1091/mbc.E18-07-0438 (2019).
214. Cowan, J. R. *et al.* SOS1 gain-of-function variants in dilated cardiomyopathy. *Circ. Genom. Precis Med.* **13**(4), e002892. https://doi.org/10.1161/CIRCGEN.119.002892 (2020).
215. Yang, X., Li, X., Lin, Q. & Xu, Q. Up-regulation of microRNA-203 inhibits myocardial fibrosis and oxidative stress in mice with diabetic cardiomyopathy through the inhibition of PI3K/Akt signaling pathway via PIK3CA. *Gene* **715**, 143995. https://doi.org/10.1016/j.gene.2019.143995 (2019).
216. Schmidt, A. *et al.* Severely altered guanidino compound levels, disturbed body weight homeostasis and impaired fertility in a mouse model of guanidinoacetate *N*-methyltransferase (GAMT) deficiency. *Hum. Mol. Genet.* **13**(9), 905–921. https://doi.org/10.1093/hmg/ddh112 (2004).
217. Liu, C. *et al.* Identifying RBM47, HCK, CD53, TYROBP, and HAVCR2 as hub genes in advanced atherosclerotic plaques by network-based analysis and validation. *Front. Genet.* **11**, 602908. https://doi.org/10.3389/fgene.2020.602908 (2021).
218. Zhu, W. S. *et al.* Hsp90aa1: A novel target gene of miR-1 in cardiac ischemia/reperfusion injury. *Sci. Rep.* **6**, 24498. https://doi.org/10.1038/srep24498 (2016).

219. Qian, X. *et al.* Enhanced autophagy in GAB1-deficient vascular endothelial cells is responsible for atherosclerosis progression. *Front. Physiol.* **11**, 559396. https://doi.org/10.3389/fphys.2020.559396 (2021).
220. Cannavo, A. *et al.* β1-adrenergic receptor and sphingosine-1-phosphate receptor 1 (S1PR1) reciprocal downregulation influences cardiac hypertrophic response and progression to heart failure: protective role of S1PR1 cardiac gene therapy. *Circulation* **128**(15), 1612–1622. https://doi.org/10.1161/CIRCULATIONAHA.113.002659 (2013).
221. Stobdan, T., Zhou, D., Williams, A. T., Cabrales, P. & Haddad, G. G. Cardiac-specific knockout and pharmacological inhibition of Endothelin receptor type B lead to cardiac resistance to extreme hypoxia. *J. Mol. Med. (Berl).* **96**(9), 975–982. https://doi.org/10.1007/s00109-018-1673-2 (2018).
222. Song, K. Y., Zhang, X. Z., Li, F. & Ji, Q. R. Silencing of ATP2B1-AS1 contributes to protection against myocardial infarction in mouse via blocking NFKBIA-mediated NF-κB signalling pathway. *J. Cell Mol. Med.* **24**(8), 4466–4479. https://doi.org/10.1111/jcmm.15105 (2020).
223. Yang, B. *et al.* The muscle-specific microRNA miR-1 regulates cardiac arrhythmogenic potential by targeting GJA1 and KCNJ2 [published correction appears in Nat Med. 2011 Dec;17(12):1693]. *Nat. Med.* **13**(4), 486–491. https://doi.org/10.1038/nm1569 (2007).
224. Wan, X. *et al.* MicroRNA-128-1-5p attenuates myocardial ischemia/reperfusion injury by suppressing Gadd45g-mediated apoptotic signaling. *Biochem. Biophys. Res. Commun.* **530**(1), 314–321. https://doi.org/10.1016/j.bbrc.2020.07.009 (2020).
225. Guo, Y. *et al.* PHLDA1 is a new therapeutic target of oxidative stress and ischemia reperfusion-induced myocardial injury. *Life Sci.* **245**, 117347. https://doi.org/10.1016/j.lfs.2020.117347 (2020).
226. Lai, J. H. *et al.* Mitochondrial protein CMPK2 regulates IFN alpha-enhanced foam cell formation, potentially contributing to premature atherosclerosis in SLE. *Arthritis Res. Ther.* **23**(1), 120. https://doi.org/10.1186/s13075-021-02470-6 (2021).
227. Wang, D. *et al.* A genetic variant in FIGN gene reduces the risk of congenital heart disease in Han Chinese populations. *Pediatr. Cardiol.* **38**(6), 1169–1174. https://doi.org/10.1007/s00246-017-1636-3 (2017).
228. Vega, A. L., Tester, D. J., Ackerman, M. J. & Makielski, J. C. Protein kinase A-dependent biophysical phenotype for V227F-KCNJ2 mutation in catecholaminergic polymorphic ventricular tachycardia. *Circ. Arrhythm Electrophysiol.* **2**(5), 540–547. https://doi.org/10.1161/CIRCEP.109.872309 (2009).
229. Minoretti, P. *et al.* A novel Val734Ile variant in the ABCC9 gene associated with myocardial infarction. *Clin. Chim Acta.* **370**(1–2), 124–128. https://doi.org/10.1016/j.cca.2006.02.007 (2006).
230. Zhuo, C., Jiang, R., Lin, X. & Shao, M. LncRNA H19 inhibits autophagy by epigenetically silencing of DIRAS3 in diabetic cardiomyopathy. *Oncotarget* **8**(1), 1429–1437. https://doi.org/10.18632/oncotarget.13637 (2017).
231. Edin, M. L. *et al.* Epoxide hydrolase 1 (EPHX1) hydrolyzes epoxyeicosanoids and impairs cardiac recovery after ischemia. *J. Biol. Chem.* **293**(9), 3281–3292. https://doi.org/10.1074/jbc.RA117.000298 (2018).
232. Sack, M. N. Rab4a signaling unmasks a pivotal link between myocardial homeostasis and metabolic remodeling in the diabetic heart. *J. Mol. Cell Cardiol.* **49**(6), 908–910. https://doi.org/10.1016/j.yjmcc.2010.09.002 (2010).
233. Yan, B. & Wang, J. UBIAD1 expression is associated with cardiac hypertrophy in spontaneously hypertensive rats. *Mol. Med. Rep.* **19**(1), 651–659. https://doi.org/10.3892/mmr.2018.9693 (2019).
234. Ng, K. *et al.* An international multicenter evaluation of inheritance patterns, arrhythmic risks, and underlying mechanisms of CASQ2-catecholaminergic polymorphic ventricular tachycardia. *Circulation* **142**(10), 932–947. https://doi.org/10.1161/CIRCULATIONAHA.120.045723 (2020).
235. Linschoten, M. *et al.* Truncating titin (TTN) variants in chemotherapy-induced cardiomyopathy. *J. Card. Fail.* **23**(6), 476–479. https://doi.org/10.1016/j.cardfail.2017.03.003 (2017).
236. Noori, M. R., Zhang, B. & Pan, L. Is KCNH1 mutation related to coronary artery ectasia. *BMC Cardiovasc. Disord.* **19**(1), 296. https://doi.org/10.1186/s12872-019-01276-4 (2019).
237. Hu, J. *et al.* RBFox2-miR-34a-Jph2 axis contributes to cardiac decompensation during heart failure. *Proc. Natl. Acad. Sci. U. S. A.* **116**(13), 6172–6180. https://doi.org/10.1073/pnas.1822176116 (2019).
238. Omede, A. *et al.* The oxoglutarate receptor 1 (OXGR1) modulates pressure overload-induced cardiac hypertrophy in mice. *Biochem. Biophys. Res. Commun.* **479**(4), 708–714. https://doi.org/10.1016/j.bbrc.2016.09.147 (2016).
239. Bi, H. L. *et al.* Inhibition of UCHL1 by LDN-57444 attenuates Ang II-Induced atrial fibrillation in mice. *Hypertens. Res.* **43**(3), 168–177. https://doi.org/10.1038/s41440-019-0354-z (2020).
240. Zhao, L. *et al.* Circulating Serpina3 levels predict the major adverse cardiac events in patients with myocardial infarction. *Int. J. Cardiol.* **300**, 34–38. https://doi.org/10.1016/j.ijcard.2019.08.034 (2020).
241. Zhou, K., Li, Y., Xu, Y. & Guo, R. Circulating matrix metalloproteinase-28 levels are related to GRACE scores and short-term outcomes in patients with acute myocardial infarction. *Biomed. Res. Int.* **2020**, 9206703. https://doi.org/10.1155/2020/9206703 (2020).
242. Wang, X. *et al.* Critical role of ADAMTS2 (a disintegrin and metalloproteinase with thrombospondin motifs 2) in cardiac hypertrophy induced by pressure overload. *Hypertension* **69**(6), 1060–1069. https://doi.org/10.1161/HYPERTENSIONAHA.116.08581 (2017).
243. Timur, A. A. *et al.* P2RY1 and P2RY12 polymorphisms and on-aspirin platelet reactivity in patients with coronary artery disease. *Int. J. Lab. Hematol.* **34**(5), 473–483. https://doi.org/10.1111/j.1751-553X.2012.01420.x (2012).
244. Huang, R. *et al.* miR-532-3p-CSF2RA axis as a key regulator of vulnerable atherosclerotic plaque formation. *Can. J. Cardiol.* **36**(11), 1782–1794. https://doi.org/10.1016/j.cjca.2019.12.018 (2020).
245. Mo, X. G. *et al.* NCF2, MYO1F, S1PR4, and FCN1 as potential noninvasive diagnostic biomarkers in patients with obstructive coronary artery: A weighted gene co-expression network analysis. *J. Cell Biochem.* **120**(10), 18219–18235. https://doi.org/10.1002/jcb.29128 (2019).
246. Tregouet, D. A. *et al.* SELPLG gene polymorphisms in relation to plasma SELPLG levels and coronary artery disease. *Ann. Hum. Genet.* **67**(Pt 6), 504–511. https://doi.org/10.1046/j.1529-8817.2003.00053.x (2003).
247. Li, W. *et al.* SAMHD1 gene mutations are associated with cerebral large-artery atherosclerosis. *Biomed. Res. Int.* **2015**, 739586. https://doi.org/10.1155/2015/739586 (2015).
248. Guicheney, P., Soliman, H., Launay, J. M., Dreux, C. & Meyer, P. Circulating monoamine oxidase B and phenolsulfotransferase activities in essential hypertensive patients. *Clin. Exp. Hypertens. A.* **10**(4), 533–544. https://doi.org/10.3109/10641968809033907 (1988).
249. Selvarajah, V. *et al.* Novel mechanism for buffering dietary salt in humans: Effects of salt loading on skin sodium, vascular endothelial growth factor C, and blood pressure. *Hypertension* **70**(5), 930–937. https://doi.org/10.1161/HYPERTENSIONAHA.117.10003 (2017).
250. Zhao, Q., Sun, H., Yin, L. & Wang, L. miR-126a-5p-Dbp and miR-31a-Crot/Mrpl4 interaction pairs crucial for the development of hypertension and stroke. *Mol. Med. Rep.* **20**(5), 4151–4167. https://doi.org/10.3892/mmr.2019.10679 (2019).
251. Sun, L. *et al.* miR-182-3p/Myadm contribute to pulmonary artery hypertension vascular remodeling via a KLF4/p21-dependent mechanism. *Theranostics.* **10**(12), 5581–5599. https://doi.org/10.7150/thno.44687 (2020).
252. Zhou, J. J. *et al.* Nestin represents a potential marker of pulmonary vascular remodeling in pulmonary arterial hypertension associated with congenital heart disease. *J. Mol. Cell Cardiol.* **149**, 41–53. https://doi.org/10.1016/j.yjmcc.2020.09.005 (2020).
253. Baptista, R. *et al.* MicroRNA-424(322) as a new marker of disease progression in pulmonary arterial hypertension and its role in right ventricular hypertrophy by targeting SMURF1. *Cardiovasc. Res.* **114**(1), 53–64. https://doi.org/10.1093/cvr/cvx187 (2018).

254. Zicha, J. *et al.* Pharmacogenetic analysis of captopril effects on blood pressure: possible role of the Ednrb (endothelin receptor type B) candidate gene. *Physiol. Res.* **63**(2), 263–265. https://doi.org/10.33549/physiolres.932732 (2014).
255. Zou, L. *et al.* Identification of a low frequency missense mutation in MUC6 contributing to pulmonary artery hypertension by whole-exome sequencing. *Pulm. Circ.* **8**(3), 2045894018794374. https://doi.org/10.1177/2045894018794374 (2018).
256. Sun, S. *et al.* A TOR2A gene product: Salusin-β contributes to attenuated vasodilatation of spontaneously hypertensive rats. *Cardiovasc. Drugs Ther.* **35**(1), 125–139. https://doi.org/10.1007/s10557-020-06983-1 (2021).
257. Eaaswarkhanth, M., Dos Santos, A. L. C., Gokcumen, O., Al-Mulla, F. & Thanaraj, T. A. Genome-wide selection scan in an Arabian peninsula population identifies a TNKS haplotype linked to metabolic traits and hypertension. *Genome Biol. Evol.* **12**(3), 77–87. https://doi.org/10.1093/gbe/evaa033 (2020).
258. Wang, J., Yang, K. & Yuan, J. X. NEDD9, a hypoxia-upregulated mediator for pathogenic platelet-endothelial cell interaction in pulmonary hypertension. *Am. J. Respir. Crit. Care Med.* https://doi.org/10.1164/rccm.202101-0007ED.10.1164/rccm.202101-0007ED (2021).
259. Nitta, C. H. *et al.* Role of ASIC1 in the development of chronic hypoxia-induced pulmonary hypertension. *Am. J. Physiol. Heart Circ. Physiol.* **306**(1), H41–H52. https://doi.org/10.1152/ajpheart.00269.2013 (2014).
260. Omura, J. *et al.* ADAMTS8 promotes the development of pulmonary arterial hypertension and right ventricular failure: A possible novel therapeutic target. *Circ. Res.* **125**(10), 884–906. https://doi.org/10.1161/CIRCRESAHA.119.315398 (2019).
261. White, Z. *et al.* Angiotensin II receptor blocker losartan exacerbates muscle damage and exhibits weak blood pressure-lowering activity in a dysferlin-null model of Limb-Girdle muscular dystrophy type 2B. *PLoS One* **14**(8), e0220903. https://doi.org/10.1371/journal.pone.0220903 (2019).
262. Amlal, H., Xu, J., Barone, S., Zahedi, K. & Soleimani, M. The chloride channel/transporter Slc26a9 regulates the systemic arterial pressure and renal chloride excretion. *J. Mol. Med. (Berl).* **91**(5), 561–572. https://doi.org/10.1007/s00109-012-0973-1 (2013).
263. Le Ribeuz, H. *et al.* In vivo miR-138-5p inhibition alleviates monocrotaline-induced pulmonary hypertension and normalizes pulmonary KCNK3 and SLC45A3 expression. *Respir. Res.* **21**(1), 186. https://doi.org/10.1186/s12931-020-01444-7 (2020).
264. Berg, T. M-currents (Kv7.2–7.3/KCNQ2-KCNQ3) are responsible for dysfunctional autonomic control in hypertensive rats. *Front. Physiol.* **7**, 584. https://doi.org/10.3389/fphys.2016.00584 (2016).
265. Yang, S. *et al.* Experimental study of the protective effects of SYVN1 against diabetic retinopathy. *Sci. Rep.* **5**, 14036. https://doi.org/10.1038/srep14036 (2015).
266. Zhang, Z. Z., Qin, X. H. & Zhang, J. MicroRNA-183 inhibition exerts suppressive effects on diabetic retinopathy by inactivating BTG1-mediated PI3K/Akt/VEGF signaling pathway. *Am. J. Physiol. Endocrinol. Metab.* **316**(6), E1050–E1060. https://doi.org/10.1152/ajpendo.00444.2018 (2019).
267. Wang, J. *et al.* Association of CFH and CFB gene polymorphisms with retinopathy in type 2 diabetic patients. *Mediat. Inflamm.* **2013**, 748435. https://doi.org/10.1155/2013/748435 (2013).
268. Chen, Y. *et al.* Association of the gene polymorphisms of BMPR2, ACVRL1, SMAD9 and their interactions with the risk of essential hypertension in the Chinese Han population. *Biosci. Rep.* **39**(1), BSR20181217. https://doi.org/10.1042/BSR20181217 (2019).
269. Gregg, T. *et al.* Obesity-dependent CDK1 signaling stimulates mitochondrial respiration at complex I in pancreatic β-cells. *J. Biol. Chem.* **294**(12), 4656–4666. https://doi.org/10.1074/jbc.RA118.006085 (2019).
270. Karere, G. M. *et al.* Sex differences in microRNA expression and cardiometabolic risk factors in hispanic adolescents with obesity. *J. Pediatr.* https://doi.org/10.1016/j.jpeds.2021.03.070 (2021).
271. Costantino, S. *et al.* Obesity-induced activation of JunD promotes myocardial lipid accumulation and metabolic cardiomyopathy. *Eur. Heart J.* **40**(12), 997–1008. https://doi.org/10.1093/eurheartj/ehy903 (2019).
272. Westergren, R. *et al.* Overexpression of Foxf2 in adipose tissue is associated with lower levels of IRS1 and decreased glucose uptake in vivo. *Am. J. Physiol. Endocrinol. Metab.* **298**(3), E548–E554. https://doi.org/10.1152/ajpendo.00395.2009 (2010).
273. Catanzaro, G. *et al.* Circulating microRNAs in elderly type 2 diabetic patients. *Int. J. Endocrinol.* **2018**, 6872635. https://doi.org/10.1155/2018/6872635 (2018).
274. Demirsoy, İH. *et al.* Profiles of circulating MiRNAs following metformin treatment in patients with type 2 diabetes. *J. Med. Biochem.* **37**(4), 499–506. https://doi.org/10.2478/jomb-2018-0009 (2018).
275. Li, L., Bai, Y., Du, R., Tang, L. & Li, L. The role of Smad4 in the regulation of insulin resistance, inflammation and cell proliferation in HTR8-Svneo cells. *Cell Biochem. Funct.* **39**(1), 126–138. https://doi.org/10.1002/cbf.3594 (2021).
276. Wang, N. *et al.* Astragalus polysaccharides decreased the expression of PTP1B through relieving ER stress induced activation of ATF6 in a rat model of type 2 diabetes. *Mol. Cell Endocrinol.* **307**(1–2), 89–98. https://doi.org/10.1016/j.mce.2009.03.001 (2009).
277. Onrat, S. T., Onrat, E., Ercan Onay, E., Yalım, Z. & Avşar, A. The genetic determination of the differentiation between ischemic dilated cardiomyopathy and idiopathic dilated cardiomyopathy. *Genet. Test Mol. Biomark.* **22**(11), 644–651. https://doi.org/10.1089/gtmb.2018.0188 (2018).
278. Huang, C. Y. *et al.* Inhibition of HSF2 SUMOylation via MEL18 upregulates IGF-IIR and leads to hypertension-induced cardiac hypertrophy. *Int. J. Cardiol.* **257**, 283–290. https://doi.org/10.1016/j.ijcard.2017.10.102 (2018).
279. Mendes-Silva, A. P. *et al.* Shared biologic pathways between alzheimer disease and major depression: A systematic review of microRNA expression studies. *Am. J. Geriatr. Psychiatry.* **24**(10), 903–912. https://doi.org/10.1016/j.jagp.2016.07.017 (2016).
280. Sakurai, A. *et al.* Involvement of Elf3 on Smad3 activation-dependent injuries in podocytes and excretion of urinary exosome in diabetic nephropathy. *PLoS One* **14**(5), e0216788. https://doi.org/10.1371/journal.pone.0216788 (2019).
281. Yan, L. *et al.* The Y chromosome regulates BMPR2 expression via SRY: A possible reason "why" fewer males develop pulmonary arterial hypertension. *Am. J. Respir. Crit. Care Med.* **198**(12), 1581–1583. https://doi.org/10.1164/rccm.201802-0308LE (2018).

Acknowledgements

I thank Anders Roger Hedin, Uppsala University, Clinical immunology, Olle Korsgren, Uppsala, Uppland, Sweden, very much, the author who deposited their profiling by high throughput sequencing dataset GSE162689, into the public GEO database.

Author contributions

M.P.—Methodology and validation. B.V.—Writing original draft, and review and editing. S.K.—Formal analysis and resources. C.V.—Software and investigation. S.K.—Supervision and resources.

Competing interests

The authors declare no competing interests.

Additional information

Supplementary Information The online version contains supplementary material available at https://doi.org/10.1038/s41598-022-13291-1.

Correspondence and requests for materials should be addressed to C.V.